

CNN-Based Action Recognition and Pose Estimation for Classifying Animal Behavior from Videos: A Survey

MICHAEL PÉREZ and COREY TOLER-FRANKLIN, University of Florida, USA

Classifying the behavior of humans or animals from videos is important in biomedical fields for understanding brain function and response to stimuli. Action recognition, classifying activities performed by one or more subjects in a trimmed video, forms the basis of many of these techniques. Deep learning models for human action recognition have progressed significantly over the last decade. Recently, there is an increased interest in research that incorporates deep learning-based action recognition for animal behavior classification. However, human action recognition methods are more developed. This survey presents an overview of human action recognition and pose estimation methods that are based on convolutional neural network (CNN) architectures and have been adapted for animal behavior classification in neuroscience. Pose estimation, estimating joint positions from an image frame, is included because it is often applied before classifying animal behavior. First, we provide foundational information on algorithms that learn spatiotemporal features through 2D, two-stream, and 3D CNNs. We explore motivating factors that determine optimizers, loss functions and training procedures, and compare their performance on benchmark datasets. Next, we review animal behavior frameworks that use or build upon these methods, organized by the level of supervision they require. Our discussion is uniquely focused on the technical evolution of the underlying CNN models and their architectural adaptations (which we illustrate), rather than their usability in a neuroscience lab. We conclude by discussing open research problems, and possible research directions. Our survey is designed to be a resource for researchers developing fully unsupervised animal behavior classification systems of which there are only a few examples in the literature.

CCS Concepts: • **Computing methodologies** → **Neural networks**.

Additional Key Words and Phrases: Deep Learning, Action Recognition, Pose Estimation, Behavior Phenotyping, Levels of Supervision

1 INTRODUCTION

This survey presents a comprehensive overview of CNN architectures for human action recognition and human pose estimation from videos. The paper traces the development and adaptations of the subset of networks that have been extended for animal behavior classification. Action recognition aims to identify and classify the activity in a trimmed video. The output of an action recognition algorithm is a set of class labels for each trimmed video. When the class label is one of a set of pre-defined expressions that occur in response to a stimuli (behavior) [32], the task is behavior classification. Pose estimation is the task of determining a subject's position and orientation in an image frame. Pose-based action recognition methods use pose estimation predictions (image frame coordinates) to classify body movements. Pose estimation may be used to identify joint positions before classifying behavior. Action recognition is critical for analyzing motion in videos for disciplines such as robotics, security, and biomedical engineering. These methods use labels. Because manual labeling is time consuming, and introduces human bias and reproducibility issues, there is a growing interest in

Authors' address: Michael Pérez; Corey Toler-Franklin, ctoler@cise.ufl.edu, University of Florida, USA.

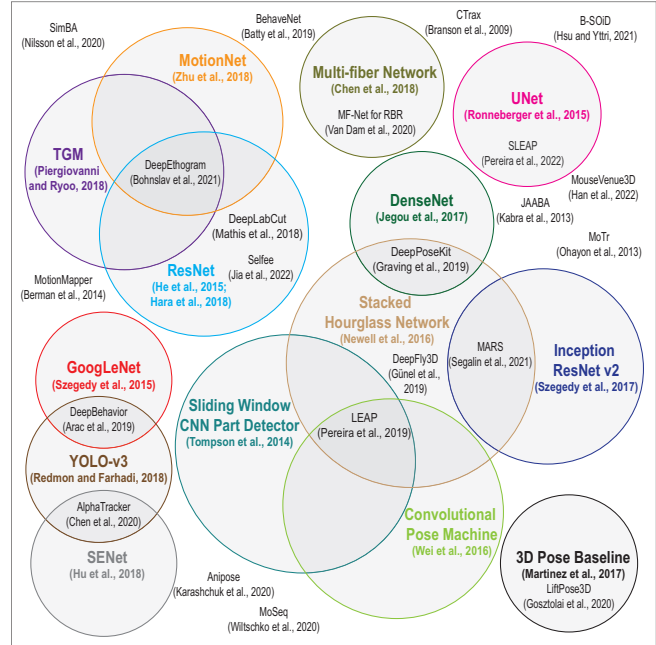


Fig. 1. CNN-based Animal Behavior Classification Frameworks and Animal Pose Estimation and Tracking Methods Organized by the Neural Network Architectures They Build Upon. Representative Examples Shown.

developing action recognition methods for fully unsupervised behavior classification that have less complex systems. A fully unsupervised method would not require labels, hand-crafted features, or additional pose estimation steps. This survey reviews CNN-based human action recognition and pose estimation methods and their extensions to animal behavior classification with a particular focus on open problems with unsupervised animal behavior classification in neuroscience.

Our contributions include:

- (1) A review of 2D, two stream and 3D CNNs that detect and analyze spatio-temporal features in videos for action recognition and pose estimation (Sections 3 and 4), including open challenges, design decisions, key contributions, and performance on benchmark datasets (Tables 4 and 5). The review focuses on the subset of methods that have extensions for classifying animal behavior.
- (2) An organizational strategy for categorizing a representative set of animal behavior classification frameworks by the level of supervision they require, considering their dependency on handcrafted features, labels, pose estimation and learning

- strategies (Section 5.4). Key contributions and performance on benchmark datasets are summarized (Tables 7, 8, and 9).
- (3) Illustrations that permit visual comparison of animal behavior classification frameworks, including system components like pose estimation techniques, neural network architectures and dimensionality reduction and clustering algorithms (Figures 9, 10 11). Diagrams that show commonalities between underlying CNN architectures (Figures 1, 4), and relationships with the human action recognition and pose estimation methods they build upon (Figure 7).
 - (4) A discussion of opportunities to develop or extend action recognition methods motivated by open problems with unsupervised animal behavior classification.

1.1 Motivation

Action recognition is an important research area in computer vision that continues to experience significant growth. This is due in part to its broad application in fields such as robotics, security, and biomedical engineering for tasks such as human-robot collaboration [97], surveillance [5], and behavior analysis [4, 32, 139]. Large publicly available video datasets [82] with high inter-class variability have facilitated the development of deep learning algorithms for video classification that are more robust and effective. However, open problems remain.

This paper focuses on action recognition methods that use CNNs to learn spatio-temporal features from videos. Spatio-temporal features are key points that exhibit spatial variations in color intensities within a frame, and temporal variation between frames. Neural networks detect these features and use them to classify video clips. Such features may be learned through network architectures that have both a spatial stream that operates on individual frames, and a temporal stream that operates on motion information. Other modifications add a temporal dimension to the filters and pooling kernels to create 3D CNNs.

Action recognition algorithms operate on trimmed videos. These trimmed videos contain one action instance. Untrimmed videos are long unsegmented videos, containing multiple action instances [159] (Figure 2). Action detection (localization, or spotting) is a related research area that locates actions of interest in space and (or) time in both trimmed and untrimmed videos. Before classifying the actions in an untrimmed video, the start and end time of each action is determined. Many classification frameworks we review in Section 5.4 operate on untrimmed videos. A small number may even incorporate networks inspired by action detection. However, they generally produce per-frame labels, without the complexities of an additional temporal action detection [159] step to segment videos. For this reason, we do not include action detection in our review. DeepEthogram [14] is an interesting example that demonstrates that action recognition and action detection are highly related. The pipeline uses a CNN developed for action recognition to estimate motion features, and then classifies the spatial and motion features in each frame using a network designed for action detection. The result is a per-frame set of behavior class labels.

Our review includes three types of learning models, categorized by the training data they operate on: *supervised* that require labeled

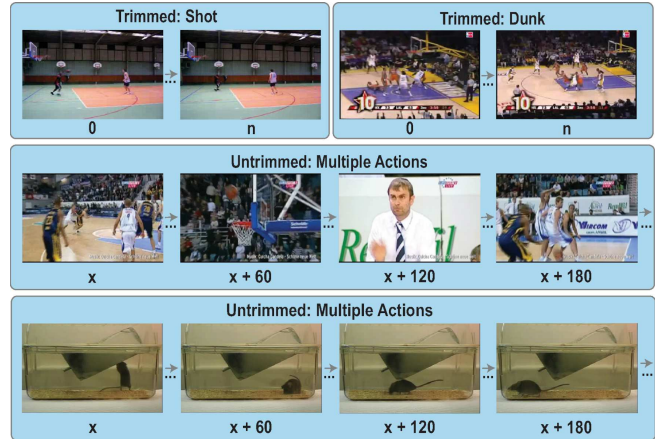


Fig. 2. Trimmed and Untrimmed Videos: (top row) The first and last frames from clipped videos of (left) a basketball dunk and (right) a basketball shot from UCF101 [143]. (middle row) Four frames 60 frames apart from an untrimmed video from THUMOS14 [75]. (bottom row) Four frames 60 frames apart from a untrimmed animal behavior dataset [72].

data, *semi-supervised* that use both labeled and unlabeled data, and *unsupervised* that operate on unstructured data without labels. Figure 2 (top row) shows class labels for *shot* and *dunk*. Figure 2 (bottom row, left to right) shows animal behavior classification labels for *rear*, *walk*, *walk*, *walk*. The label *rear* indicates that the animal stands on hind legs.

Most methods presented in this review require some level of supervision. However, using predefined labels is limiting, as micro-scale actions that are not in the labeled dataset but exist in the unstructured data, may go undetected. Direct processing on raw pixels would enable fewer processing steps, without the need for hand-crafted features to produce consistent poses for different subjects.

There are many challenges with action recognition from videos. It is challenging to trace the motion of body parts which are occluded in intermittent frames. Artifacts from variations in lighting or varying parameters from camera or devices (that have different imaging quality and frame rates) add additional challenges. Many pose-based systems do not generalize well to *in-the-wild* conditions.

Behavior analysis is important [2, 109] with many real-world applications. Recent projects extend human action recognition for detecting and interpreting behavior in small animals. Additional challenges exist in this domain [2]. Tracking multiple subjects that have identical appearance is challenging, often requiring specialized tracking devices that are distracting. Many systems incorporate several machine learning tasks such as object detection, pixel-wise segmentation, and dimensionality reduction. Thus, classification systems are often complex, requiring many processing steps. We present an organizational strategy for animal behavior classification that considers system components and learning strategies in addition to inputs.

There is a significant number of CNN-based action recognition and pose estimation methods for both human and animal activity recognition. This enables a thorough review of the subject.

Relation to Other Surveys: To our knowledge, this is the only survey with an organizational structure for examining commonalities between the neural network architectures of the related tasks of human action recognition and pose estimation (Figure 1) in the context of their extensions for animal behavior classification (Figure 7). Our survey presents a novel taxonomy for animal behavior classification frameworks that is more detailed and provides a broader range of supervision levels that are not considered in other work [10]. We also include recent work with unsupervised animal behavior classification systems which are not expounded upon in other reviews.

Surveys on human pose estimation [28, 177] and action recognition are generally handled separately, and often cover a broad range of network architectures. Zheng et. al. [177] provide a systematic review of deep learning-based 2D and 3D human pose estimation methods since 2014, while Zhu and colleagues [181] offer a comprehensive survey of deep learning methods for video action recognition. Other reviews on these topics target specific network architectures. Recently, transformers [95, 181] have become the model of choice for processing sequential data. The following surveys cover transformers for action recognition [181] and pose estimation [95].

A related body of work reviews animal behavior classification models in neuroscience and computational ethology which is the study of animal behavior [2]. These reviews cover many topics including measuring animal behavior across scales [10], machine learning for animal activity recognition [84], advances in 3D behavioral tracking [106] for full pose measurements, monitoring with wearable devices [84], and behavior profiling [166]. We focus on small laboratory animals in methods that do not require wearable tracking devices.

Many surveys in neuroscience focus on the usability of these methods as tools in a lab [109]. A 2021 review [166] evaluates behavior analysis approaches. We trace the technical development of the underlying neural network architectures.

Other surveys have proposed a taxonomy for animal behavior classification systems. One proposal [10] uses a dynamical representation of behavior that describes how the measured postural time-series are changing. Straightforward approaches [11, 72, 165] manually create features which are fed to a supervised classifier or a clustering algorithm. The author argues that a dynamical representation should be produced naturally from pose dynamics in an unsupervised manner [10].

2 BACKGROUND

We begin with definitions, terms, and background information that support the paper discussion.

Neural networks are integral to most frameworks in our review. Here we describe basic operations of a feedforward neural network. Given a function, $y = f^*(x)$ that maps an input vector x to an output label y , a feedforward neural network defines a mapping

$y = f(x, \theta)$, and learns the values of θ that yield the best approximation of f^* . Activation functions are computed at each node using function outputs from nodes at lower levels in an acyclic graph. Activation functions introduce non-linearities to improve performance on complex datasets. The rectified linear unit (ReLU) [173] function, $f(x) = \max(0, x)$ is the default activation in feedforward networks. During training, input observations x propagate forward through network layers, producing an output prediction \hat{y} and a scalar cost $J(\theta)$. Backpropagation allows cost information to flow backwards through the network for use in optimization methods (like stochastic gradient descent) that minimize $J(\theta)$. Activation functions should avoid linearities, saturation and vanishing gradients. The leaky ReLU function [104] is a modified ReLU function with a small slope for negative values that permits non-zero gradients, even when the unit is inactive. This avoids vanishing gradients that inhibit learning.

Optimizations can improve network efficiency, increase classification accuracy, and reduce adverse effects like overfitting. Architectural improvements also provide regularization within a network to address issues like vanishing gradients.

Advantages of Deep Networks: It has been shown empirically that, although deeper networks are harder to optimize, they require fewer parameters and generalize better than shallow networks [51].

Regularization is a technique that modifies a learning algorithm to reduce generalization error so that the model performs well on unseen data distributions.

Batch normalization scales and centers inputs to normalize them for faster, more stable training.

Ensemble Methods combine predictions of several neural networks to reduce test error at the expense of some additional computation costs.

2.1 Network Architectures

Convolutional Neural Networks (CNNs): [92] use convolution (rather than matrix operations) in at least one layer. CNNs are regularized multi-layer perceptrons [110] that leverage the spatial structure inherent in grid-like structures (like images) for regularization, through local filters, convolutions, and max-pooling layers. Advancements in GPU hardware have allowed CNNs to scale to networks with millions of parameters, improving state-of-the-art image classification and object recognition. AlexNet [88] was the first CNN to achieve state-of-the-art results on the ImageNet [36] dataset, a benchmark dataset used for a variety of deep learning challenges. The network is based on LeNet-5 [93]. VGGNet [142] improves upon AlexNet by using smaller convolutional filters (3×3) and increased network depth to support between 16 to 19 layers.

Inception [148] was designed to improve utilization of computing resources within a network by using 1×1 convolutions and improved multi-scale processing. The process connects auxiliary networks to intermediate layers to encourage discrimination in the

lower layers of a CNN. The auxiliary networks are discarded at test time. The GoogLeNet 22-layer network is a notable example that won the 2014 ImageNet challenge. Other examples like Inception-v3 [149] improve upon the original Inception architecture by factorizing 5×5 and 7×7 convolutions into multiple smaller, more efficient convolutional operations and incorporating batch normalization.

Fast R-CNN is a deep CNN designed for object recognition that extends the Region-Based Convolutional Neural Network (RCNN).

Autoencoder: A neural network designed for dimensionality reduction in which an encoder learns a compressed feature representation from unlabeled data. The decoder validates the representation by attempting to reconstruct the original data from the features.

Residual Neural Networks (ResNets) [58] utilize residual blocks with skip connections to jump over layers that are not updated to allow for better gradient to flow, mitigating the vanishing gradient problem. These architectural modifications permit deeper networks. The results improved upon VGGNet in the ImageNet challenge using a network with up to 152 layers.

YOLOv3 (You Only Look Once) [134] is a CNN architecture designed for fast object detection that has 53 convolutional layers and uses residual blocks [58]. The YOLO family of models is not proposal-based and frames object detection as a regression problem that predicts bounding box coordinates and class probabilities given image pixels.

Recurrent Neural Networks (RNNs): These methods process sequential or time-series data. Cycles in the graph allow output from one layer to be fed back as input to another layer.

Transformers [95, 181] are neural networks with self-attention [164] that operate on sequential data in parallel, without the need for recurrence (found in RNN-based models [9, 103]).

2.2 General Classification and Training Methods

Temporal Random Forest Classifier An extension of a random forest to the multi-frame case.

Hand-crafted Features are created by manual feature engineering. They are usually dataset dependent and do not generalize well. Neural networks, on the other hand, detect features automatically from unstructured data.

Active Learning: Semi-supervised classification of pose features as behavior labels employs unsupervised and supervised learning to minimize the number of behavioral labels while maximizing accuracy. Active learning approaches aim to systematically choose which samples should be labeled so that the number of samples is minimized, and the accuracy is maximized.

Contrastive Learning: A technique that increases the performance of vision tasks by *contrasting* samples against each other. The goal

is to learn attributes that are common between data classes, and attributes that make data classes different. The approach learns representations by minimizing the distance between positive data and maximizing the distance between negative data.

Transfer learning is a mechanism for training neural networks when there is insufficient data in the target domain. Transfer learning uses knowledge gained from one domain to improve generalization in a related domain. For example, in a supervised learning context, a model may be trained to classify images of one object category, and then used to classify images of another (training on cats and dogs and testing on horses and cows for example). This is useful because visual categories often share low-level features like edges and shapes. Another transfer learning technique trains a model on a large unlabeled dataset using an unsupervised learning algorithm, then fine-tunes the model on a labeled dataset with a supervised algorithm. This unsupervised pretraining is helpful as large, labeled datasets are hard to collect.

ImageNet Pre-Training: ImageNet is a benchmark dataset used for a variety of deep learning challenges including transfer learning experiments. It contains 1,431,167 images that correspond to 1,000 classes and large networks trained on this dataset have shown state-of-the-art results in the image domain. The full ImageNet dataset contains 22,000 classes, but in experiments and the ImageNet challenge 1,000 high-level categories are used. Transfer learning methods [124] that use ImageNet as a source domain have been effective for improving state-of-the-art classification results in related target domains. For example, a network trained on ImageNet was used [124] for the PASCAL Visual Objects Classes challenge [40]. Through transfer learning, deep CNNs pre-trained on ImageNet were also used for other tasks like scene recognition [38] and object recognition [49]. In Section 4, we discuss transfer learning on video datasets.

2.3 Action Recognition: Terms

Spatio-temporal Features are used to analyze changes in image structure that vary with time. Spatial interest points occur at positions of significant local variation in image intensities [100]. Spatio-temporal interest points are extensions of spatial interest points as they record significant local variation of the pixel intensity in the spatio-temporal domain of the video volume [99].

2.4 Graphical Models

Hidden Markov Model (HMM): A graphical model that represents probability distributions over sequences of observations that are produced by a stochastic process. The states of the process are hidden. The state Z_t at time t satisfies *Markov properties* and depends only on the previous state, Z_{t-1} at time $t - 1$.

Autoregressive Hidden Markov model (AR-HMM): A combination of autoregressive time-series and Hidden Markov Models.

Graph Convolution Networks extend convolution from images to graphs and have been used successfully in pose-based action recognition.

Belief Propagation is a message-passing algorithm for performing inference in graphical models.

Graphical Models for Joint Detection: Pose estimation methods may use graphical models with nodes that represent joints and edges that represent pairwise relationships between joints. Each final joint distribution is a product of unary terms which model the joint’s appearance cues, and pairwise terms which model local joint inter-connectivities. These methods examine local image patches around a joint to detect it, and to estimate the relative position of neighboring joints.

2.5 Pose Estimation: Terms

Part Affinity Fields are a set of 2D vector fields that represent the location and orientation of limbs in an image.

2.6 Pose Estimation: Evaluation Metrics

Percentage of Correct Parts (PCP) evaluates limb detection. A limb is detected if the distance between the prediction and the true limb location is within a threshold: half the limb length.

Percent of Detected Joints (PDJ) evaluates joint detection. A joint is detected if the distance between the prediction and the true joint location is within a threshold: a specified fraction of the torso diameter.

Percent of Correct Keypoints (PCK) is an accuracy metric that determines whether the distance between the predicted keypoint and the true joint location lies within a varying threshold.

3 HUMAN POSE ESTIMATION

In this section, we review CNN-based human pose estimation techniques that operate on images (Section 3.1) and videos (Section 3.2). The methods presented contribute to animal behavior classification frameworks presented in Section 5. Table 1 summarizes common benchmark image datasets used in deep learning, with pose estimation datasets indicated with bold text. The key contributions of the methods discussed are summarized in Table 4.

Human pose estimation methods generate a set of (x, y) coordinates that correspond to the position of body joints within an image frame. These predictions are used as input to pose-based action recognition methods. Using taxonomy from deep learning-based human pose estimation [177], we categorize these approaches as 2D or 3D, and single-person or multi-person. The 2D single-person methods are regression-based or detection-based. Regression-based methods regress an image to find joint locations, while detection-based methods detect body parts using heat maps. The 2D multi-person methods use top-down or bottom-up pipeline approaches. Top-down pipeline approaches use person detectors to obtain a set of bounding boxes for each person in the image before applying single-person pose estimation techniques to each bounding box to

obtain the multi-person pose estimation. Bottom-up pipeline approaches first locate all the joints of all people in an image, and then assign them to individuals. We cover 3D pose estimation from image or video input, and categorize methods as single-view/single-person, single-view/multi-person or multi-view.

Dataset	Year	Size	Classes	Joints
MNIST [93]	1998	70,000	10	-
ImageNet [36]	2009	1,431,167	1,000	-
CIFAR-10 [87]	2009	60,000	10	-
HumanEva [140]	2009	40,000	-	15
LSP [77]	2010	2,000	-	14
TFD [147]	2010	112,234	7	-
Cropped SVHN [117]	2011	630,420	10	-
LSP-extended [78]	2011	10,000	-	14
FLIC [138]	2013	5,003	-	10
FLIC-motion [70]	2015	5,003	-	10
MPII human pose [3]	2014	40,522	-	16
Human3.6M [67]	2014	3.6M	-	24
MPI-INF-3DHP [112]	2017	1.3M	-	24

Table 1. Common Benchmark datasets for Image Classification and Pose Estimation from Images. The right columns indicate whether the data has class or joint labels.

Dataset	Year	Trimmed	Size	Average Length (sec.)	Classes
CCV [76]	2011	✓	9,317	80	20
HMDB51 [46]	2011	✓	7,000	~ 5	51
UCF101 [143]	2012	✓	13.3K	~ 6	101
Sports-1M [82]	2014	✓	1.1M	~ 330	487
THUMOS14 [75]	2014	✗	5,084	233	101
ActivityNet [59]	2015	✗	9,682	[300,600]	203
Kinetics-400 [83]	2017	✓	306K	10	400
Kinetics-600 [23]	2018	✓	482K	10	600

Table 2. Common Video Benchmark Datasets

Input 64×64 color image
5×5 conv. RELU. 2×2 MaxPool. $\mathbb{R}^{16 \times 32 \times 32}$
5×5 conv. RELU. 2×2 MaxPool. $\mathbb{R}^{32 \times 16 \times 16}$
5×5 conv. RELU. now $\mathbb{R}^{16 \times 32 \times 32}$. flatten to \mathbb{R}^{8192}
FC. RELU. \mathbb{R}^{500}
FC. RELU. \mathbb{R}^{100}
FC. logistic unit. \mathbb{R}^1

Table 3. Body Part Detector Architecture [69] for Human Pose Estimation

3.1 Pose Estimation from Images

2D Single-Person Pose Estimation

Detection-Based: One of the first pose estimation techniques to apply a CNN was a two-stage filtering approach [69] for finding joint positions. The first stage generates a binary response map for each joint, applying multiple CNNs as sliding windows on overlapping areas of an image. The response map is a unary distribution representing the confidence of the joint’s presence over all pixel positions. Denoising in the second stage removes false positives by passing the CNN output through a higher-level spatial model with body pose priors computed on the training set. Prior conditional distributions for two joints (a, b) are calculated as a histogram of joint a locations given that joint b is at the image center. Similarly, a global position prior for the face is calculated using a histogram of face positions. A process similar to sum-product belief propagation [126] generates the filtered distributions for each joint given unary distributions produced by the CNNs and the prior conditional distributions.

This non-linear mapping from pixels to vector representations of articulated pose is challenging. Data loss during pooling, and high numbers of invalid poses in the training data make valid poses difficult to learn. To avoid this, a performance improvement trained multiple CNNs for independent binary joint detection, using one network for each feature. Each CNN (shown in Table 3) has a single output unit representing the probability of a joint being present in the image patch. Results were evaluated on the FLIC [138] dataset, which consists of images of Hollywood actors in front-facing poses. The percentage of correct joint predictions within a given precision radius (in pixels) is used as a quantitative metric for pose estimation accuracy. The model outperformed state-of-the-art estimation methods available at the time.

OpenPose uses a convolutional pose machine [170] to predict keypoint coordinates, and part affinity fields to determine correspondences between keypoints and subjects in the image. Convolutional Pose Machines are a sequence of CNNs that produce increasingly refined belief maps for estimating 2D pose, without a graphical model. This design enforces intermediate supervision and limits vanishing gradients. Transfer learning with pre-training on ImageNet improves performance. Predefined rules are used to determine if pose features represent specific behaviors.

Regression-based: Human pose estimation may be formulated as a continuous regression problem. DeepPose [155] regresses an image to a normalized pose vector representing body joint locations. The network input is (X, \mathbf{y}) , where X is a labeled image and $\mathbf{y} = \{\dots, y_i^T, \dots\}^T$ is the true pose vector. Each \mathbf{y}_i is the absolute image coordinates of the i th joint, where $i \in \{1, \dots, k\}$ and k is the number of joints. Each joint position must be normalized with respect to a bounding box, b , centered around the human subject to produce a normalized pose vector $N(\mathbf{y}; b) = (\dots, N(\mathbf{y}_i; b)^T, \dots)^T$.

The DeepPose CNN architecture ψ is based on AlexNet [88]. However, rather than formulate a classification problem, a linear regressor is trained to learn the parameters θ of a function $\psi(X; \theta) \in \mathbb{R}^{2k}$ such that an image X regresses to a pose prediction \mathbf{y}^* in absolute image coordinates:

$$\mathbf{y}^* = N^{-1}(\psi(N(X); \theta)) \quad (1)$$

The linear regressor is trained on the last network layer to predict a pose vector by minimizing the L_2 distance between the prediction and ground truth pose vector. The training set is first normalized as explained, yielding the following optimization problem:

$$\operatorname{argmin}_{\theta} \sum_{(X, \mathbf{y}) \in D_N} \sum_{i=1}^k \|\mathbf{y}_i - \psi_i((X, \theta))\|_2^2, \quad (2)$$

where D_N is the normalized training set:

$$D_N = \{(N(X), N(\mathbf{y})) | (X, \mathbf{y}) \in D\}. \quad (3)$$

DeepPose CNNs operate on coarse scale images at a fixed resolution (220×220 pixels), making it difficult to analyze fine image detail at the level required for precise joint localization. To address this, a cascade of pose regressors was introduced after the first stage to predict the displacement of the predicted joint locations (from prior states) to the true joint locations. Relevant parts of the image are targeted at higher resolutions for higher precision without increasing computation costs. The model was evaluated on datasets that include a variety of poses including the aforementioned FLIC dataset [138], the Leeds Sports Poses dataset (LSP) [77] of athletes participating in sports, and its extension [78]. Limb detection rates evaluated using PCP and PDJ produced state-of-the-art or better results on both metrics.

Joint Training with A Graphical Model: Hybrid methods that combine multiresolution CNNs and joint training with graphical models produce higher accuracy rates than DeepPose. These models address limitations with network capacity, overfitting, and inefficiencies caused by nonlinear mappings from image to vector space. CNNs [176] that operate on multi-resolution input, can identify a broad range of feature sizes in a single forward pass by adapting the effective receptive field within CNN layers.

Tompson et. al. [154] combined a CNN with a Markov Random Field, an undirected graph with Markov properties [115]. A multi-resolution feature representation with overlapping receptive fields was used to perform heat-map likelihood regression. Starting with an input image, a sliding window CNN generates a per-pixel heat-map of likelihoods for joint locations. The CNN was trained jointly with a graphical model. In later stages, a spatial model predicts which heat-maps contain false positives and incorrect poses. This is

done by constraining joint inter-connectivity and enforcing global pose consistency. The graph is learned implicitly without hand-crafted pose priors or graph structure [69]. The results showed improved accuracy compared to the previous state-of-the-art [69, 155] in human body pose recognition using the FLIC and LSP-extended datasets with PDJ as the evaluation metric.

A later extension [153] improved localization accuracy by recovering the precision lost due to pooling. The input image was first passed through a CNN for coarse-level pose estimation to produce initial heat maps with per-pixel likelihoods of joint positions. The heat-maps were then passed through a position refinement model to refine the pose prediction. This modification outperformed the previous state-of-the-art on the FLIC and MPII human pose [3] benchmarks. The MPII human pose dataset is comprised of 24,520 images of humans performing everyday activities collected from YouTube videos. This method outperformed previous state-of-the-art pose estimation methods [69, 154, 155] on the FLIC dataset using PCK scores. Another method uses a *Graphical Model with Image Dependent Pairwise Relations* [26] to generate input for both the unary and pairwise terms from image patches. Experiments performed on the FLIC and LSP datasets showed that this formulation improves upon DeepPose according to multiple metrics.

2D Multi-Person

There are additional challenges with pose estimation when multiple subjects interact in a video. Most early strategies for multi-person pose estimation used a two-stage inference process to first detect and then independently estimate poses. However, this method is less effective when multiple people have overlapping body parts because the same body part candidates are often assigned to multiple people.

A proposed solution, DeepCut [133], casts the joint detection and pose estimation problems as integer linear programs. DeepCut's formulation is a Joint Subset Partitioning and Labeling Problem (SPLP) that jointly infers the number of people and poses, the spatial proximity, and areas of occlusion. The solution jointly estimates the poses of all people in an image by minimizing a joint objective. A set of joint candidates is partitioned and labeled into subsets that correspond to mutually consistent joint candidates that satisfy certain constraints. Even though the problem is NP-hard, this formulation allows feasible solutions to be computed within a certain optimality gap. DeepCut adapts two CNN architectures, Fast R-CNN [48] and VGGNet [142], to generate body part candidates. Significant improvement was shown over previous methods [26, 153, 154] for both single and multi-person pose estimation according to multiple evaluation metrics on the LSP, LSP-extended, and MPII human pose datasets.

DeeperCut [66] doubled the pose estimation accuracy of DeepCut while reducing the running time by 2-3 orders of magnitude. Contributions included novel image conditioned pairwise terms between body parts that improved performance for images with multiple people, and a novel optimization method that decreased runtime while improving pose estimation accuracy. DeeperCut adapted ResNet [58], which is $8\times$ deeper than VGGNet. Experiments were conducted on both single and multiple person human pose datasets:

LSP, LSP-extended, and MPII using the PCK evaluation metric. Results yielded a new state-of-the-art in multi-person 2D pose estimation.

3D Pose Estimation

Estimating a 3D human pose from a single RGB image is a challenging problem in computer vision because it requires solving two ambiguous tasks [152]. The first task is finding the 2D location of human joints in the image. This is hard due to different camera viewpoints, occlusions, complex body shapes, and varying illumination. The second, converting the coordinates of 2D landmarks into 3D coordinates, is an ill-posed problem that requires additional information such as 3D geometric priors and other constraints. Methods for 3D pose inference from images either regress the 3D pose directly from images, or first estimate the 2D pose and then lift the coordinates into 3D using a pipeline approach. Three-dimensional human pose estimation approaches presented in the remainder of this subsection are single-view/single-person.

Regression-based: CNNs can directly regress 3D poses from images. One method, *3D Human Pose Estimation from Monocular Images* [96], jointly trains the pose regression task with a set of recognition tasks in a heterogeneous multi-task learning framework. The network was pre-trained using the recognition tasks, then refined using only the pose regression task. A *Maximum-Margin Structured Learning* technique [98] takes an image and a 3D pose as input, and produces a score that indicates whether the pose is depicted. During training a maximum-margin cost function is used to enforce a re-scaling margin between the score values of the ground truth image-pose pair and the rest of the pairs. The results showed improved performance. Overcomplete autoencoders [19] have been used to learn a high-dimensional latent pose representation. This method accounts for joint dependencies that predict 3D human poses from monocular images. The problem was also posed as a key point localization problem in a discretized 3D space [125]. In this case, a CNN is trained to predict per voxel likelihoods for each joint in the volume.

At the time, among pipeline approaches, it was unclear whether the remaining error in state-of-the-art methods was due to a limited 2D pose understanding, or from a failure to map 2D poses to 3D positions. To better understand the sources of error, the 3D human pose estimation problem was decoupled into the well-studied problems of 2D pose estimation from images and 3D pose estimation from 2D joint detections.

2D to 3D Lifting: By focusing on the latter problem, ground truth 2D joint locations can be *lifted* to 3D space using a relatively simple deep CNN. This yielded state-of-the-art results on the Human3.6M dataset [67] which consists of 3.6 million 3D human poses. The findings indicated that the remaining error in pipeline approaches for 3D pose estimation techniques stem from 2D pose analysis. Another pipeline approach [152] used a pre-learned 3D human pose model as part of the CNN architecture itself. The architecture learned to use physically plausible 3D reconstructions in its search for better 2D landmark locations. The process obtained state-of-the-art 2D

and 3D results on Human3.6M, and demonstrated the importance of considering 3D, even when solving 2D pose estimation problems.

Generalization to in-the-wild conditions: The previous pose estimation methods had low generalization to in-the-wild conditions.

Method	Year	2D/3D	Key Contribution(s)
[69]	2014	2D	<ul style="list-style-type: none"> The development of a deep CNN architecture to learn low-level features and a higher-level spatial model.
[154]	2014	2D	<ul style="list-style-type: none"> The development of a hybrid architecture that incorporates a deep CNN and a Markov Random Field that can exploit geometric constraints between body joint locations.
[26]	2014	2D	<ul style="list-style-type: none"> The development of a graphical model that uses pairwise relations to exploit how local image measurements can be used to predict joint locations and relationships. The use of a deep CNN to learn conditional probabilities for the presence of joints and their spatial relationships in image patches.
[96]	2015	3D	<ul style="list-style-type: none"> The application of a deep CNN to 3D pose estimation from monocular images. The joint training of pose regression and body part detectors.
[131]	2015	2D	<ul style="list-style-type: none"> The use of a deep CNN for estimating human pose in videos. The use of temporal information between frames to improve performance.
DeepPose [155]	2014	2D	<ul style="list-style-type: none"> The formulation of human pose estimation as a deep CNN-based regression problem. The use of a cascade of regressors to increase precision.
MoDeep [70]	2015	2D	<ul style="list-style-type: none"> The use of motion features for human pose estimation.
[153]	2015	2D	<ul style="list-style-type: none"> The introduction of a position refinement model that is trained to estimate the joint offset location in a local image region in order to improve joint localization accuracy.
DeepCut [133]	2016	2D	<ul style="list-style-type: none"> The development of a partitioning and labeling formulation of body-part predictions produced by CNN-based joint detectors. This formulation infers the number people in images, identifies occlusions, and differentiates between overlapping body parts of nearby people.
[98]	2017	3D	<ul style="list-style-type: none"> The modeling of dependencies between joints using a max-margin structured learning framework for monocular 3D pose estimation.
[19]	2016	3D	<ul style="list-style-type: none"> The use of an overcomplete autoencoder for monocular 3D pose estimation that learns a latent pose representation and models joint dependencies.
[151]	2016	3D	<ul style="list-style-type: none"> The use of motion information from video clips for 3D pose estimation and the direct regression from clips to pose in the center frame.
[125]	2017	3D	<ul style="list-style-type: none"> The discretization of 3D space around a subject for monocular 3D pose estimation. The use of a CNN to predict per voxel likelihoods for each joint.
DeeperCut [66]	2016	2D	<ul style="list-style-type: none"> The design of very deep body part detectors by building upon the ResNet architecture. The use of image conditioned pairwise terms between body parts to improve performance for images with multiple people. The development of an incremental optimization procedure that leads to speed and performance boosts.

Table 4. Summary of Pose Estimation Approaches

CNN Arch.	Method	Year	Classification Accuracy	Key Contribution(s)
2D	Slow Fusion [82]	2014	65.4%	<ul style="list-style-type: none"> The release of the Sports-1M dataset. The evaluation of CNNs for video classification and the development of slow fusion, late fusion, and early fusion.
Two-Stream	Two-Stream CNN [141]	2014	88.0%	<ul style="list-style-type: none"> The development of the two-stream architecture that incorporates spatial and temporal networks. The usage of optical flow to model movement in videos for action recognition.
	MotionNet [180]	2019	89.82%	<ul style="list-style-type: none"> The development of the MotionNet CNN that implicitly calculates optical flow between frames as a part of a two-stream architecture.
3D	C3D [156]	2015	86.7%	<ul style="list-style-type: none"> The development of an 8-layer 3D CNN that operates over 16 frames and uses filters of size $3 \times 3 \times 3$.
	$R(2+1)D$ [157]	2018	97.3%	<ul style="list-style-type: none"> The factorization of 3D convolution into 2D spatial convolution followed by 1D temporal convolution.
Two-Stream/3D	Two-Stream CNN Fusion [41]	2016	93.5%	<ul style="list-style-type: none"> The development of a two-stream architecture that uses 3D convolutional fusion and 3D pooling.
	I3D [24]	2017	98.0%	<ul style="list-style-type: none"> The usage of the Kinetics-400 dataset [24]. The development of two-stream inflated 3D CNNs that expand the filters and pooling kernels of very deep image CNNs into 3D.

Table 5. Summary of Discriminative Action Recognition Approaches and their Performance on UCF101 [143]

This is due to inherent limitations in the training datasets. A *Monocular 3D Human Pose Estimation* method [112] used transfer learning to leverage the mid and high-level features learned on existing 2D and 3D pose datasets, yielding improved performance. State-of-the-art results were obtained on the Human3.6M dataset and the HumanEva pose estimation benchmark, [140]. A new benchmark dataset, MPI-INF-3DHP [112], of indoor and outdoor scenes was presented. Transfer learning with MPI-INF-3DHP and 2D pose data yielded the best generalization to in-the-wild conditions, confirming that transfer learning is beneficial for 3D pose estimation.

3.2 Human Pose Estimation from Video

Human pose estimation approaches that operate on videos handle temporal information using techniques similar to those we cover in our discussion of human action recognition methods (Section 4). CNNs used for action recognition initially incorporated temporal information using optical flow [18] as an input motion feature [141] to a two-stream network architecture (Sections 1.1 and 4). An optical flow [18] (shown in Figure 3), is a set of displacement vector fields \mathbf{d}_t between pairs of consecutive frames t and $t + 1$. Figure 3

(top row) shows an example of the optical flow between two consecutive frames in a video of a person diving. Figure 3 (bottom row) shows a mouse walking.

Two 2D single-view/single-person pose estimation methods [69, 131], one that is detection-based and another that is regression-based, extended this idea using optical-flow maps from multiple nearby frames to predict the pose in the current frame. In a related work, *Flowing ConvNets for Human Pose Estimation* [130], when performing inference for one frame, joint positions for all neighboring frames are explicitly predicted and aligned to the corresponding frames. This is done using a dense optical flow to warp backward or forward in time. Evaluation performed on three large pose estimation datasets showed that this method outperforms the previous state-of-the-art.

MoDeep [70], and similar variants [131], improved upon DeepPose by exploiting motion as a cue for body part localization. This single-view/single-person method uses optical flow and color from multiple nearby frames as input to a multi-resolution CNN. The multi-resolution CNN was designed for estimating a human's pose in a video given an image and a set of motion features. Accuracy in high-precision regions was improved (compared to DeepPose)

by incorporating motion features, and using a translation-invariant model. Optical flow was one of several formulations considered. The FLIC-motion [70] dataset which consists of the original FLIC dataset [138] augmented with motion features, was created. MoDeep performed best on FLIC-motion compared to other state-of-the-art pose estimation methods. A related technique by Tekin et al. [19] extended a CNN architecture for pose estimation on still images [151] to operate on video. It included temporal information in the joint predictions by extracting spatio-temporal information from a sequence of frames.

4 HUMAN ACTION RECOGNITION

Now that we have introduced CNN-based pose estimation techniques, we turn our attention to action recognition methods that track motion across video frames. Figure 4 illustrates the CNN architectures discussed in this section in green. Rectangles denote architecture categories and rounded rectangles denote architectures. Architecture we discuss have been extended for animal behavior classification systems (shown in brown), that we review in Section 5.

Standard Action Recognition Methods extract features, sparse [100] or dense [167] spatio-temporal interest points, for example, and then track their displacement through frame sequences using techniques like optical flow. Improved Dense Trajectories (iDT) [168] is an example that represents motion as feature trajectories, fixed-sized descriptors computed along the paths of feature points. In this case, quantization using a k-means dictionary [89] is used to combine features. A sparse vector with stored occurrence counts of a vocabulary of local image features (bag of visual words), is then accumulated across the video. A support vector machine (SVM), or other classifier, is trained to classify the bag of visual words to discriminate video-level classes.

CNN-Based Temporal Learning: Modern deep learning methods use neural networks to detect spatio-temporal features. In our survey, we focus on CNN-based examples. While images can be scaled and cropped, and are easily processed with fixed-sized CNNs, videos are difficult to work with because they vary in temporal content. According to Karpathy et al. [82], compared to traditional machine learning approaches for action recognition [100, 167, 168], CNN-based solutions shift the engineering from feature design and extraction, to network architecture design and hyperparameter tuning.

We begin with a seminal paper by Karpathy et al. [82] that extended the connectivity of a CNN to operate in the temporal domain for video classification. The solution treats the input data as a bag of fixed-sized clips where one hundred half-second clips were randomly sampled from each video. Fusion operations are then used to extend the CNNs over the time dimension so that they operate on multiple frames and have the ability to learn spatiotemporal features from the clips. The team proposed three novel CNN connectivity patterns to fuse temporal information: Late fusion places two single-frame networks some time apart, then fuses their outputs later. Early fusion modifies the first layer to use a convolutional filter that extends in time. Slow fusion is a balance between

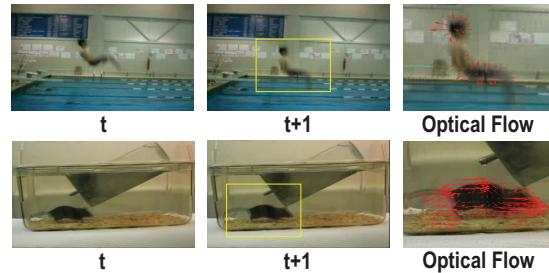


Fig. 3. (top row) Two consecutive frames and a close-up from a video of a person diving from the UCF101 [143]. (bottom row) Two consecutive frames and a close-up from a video of a mouse with a close-up from a published [72] animal behavior dataset. In each case, optical flow between the frames was calculated using MATLAB and superimposed on the second frame and close-up.

early and late fusion (Figure 5). A baseline single-frame architecture was also used to analyze the contribution of static appearance to classification accuracy.

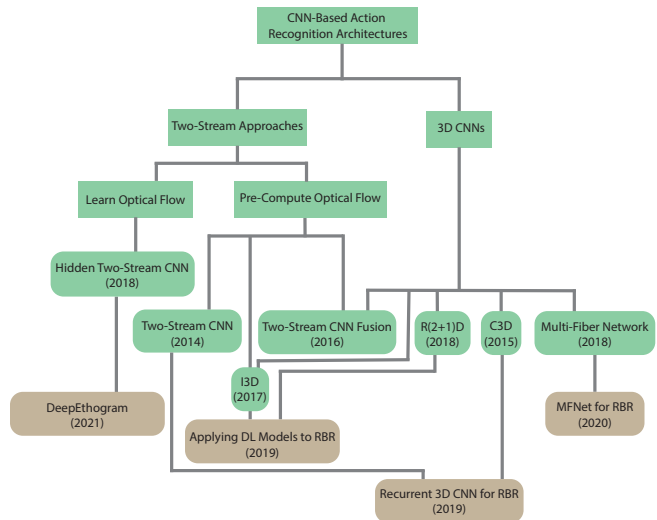


Fig. 4. CNN-based Action Recognition Architectures for Human Actions (green) and Animal Behavior Classification (brown). Rectangles denote architecture categories and rounded rectangles denote architectures.

High volume video datasets with high class variation are essential for training and testing these new architectures. The largest video datasets available at the time were CCV [76] which contains 9,317 videos and 20 classes, and UCF101 [143] which contains 13,320 videos and 101 classes. Though effective for generating early action recognition benchmarks, the scale and variety of these video datasets were not equivalent to large image datasets like ImageNet [36] (Section 2). To address this issue, the paper introduced a new benchmark action recognition dataset, the Sports-1M dataset [82] with one million trimmed YouTube videos belonging to 487 classes of sports. Each video is five minutes and 36 seconds long on average. One hundred half-second clips were randomly sampled from

each video in the Sports-1M dataset. To produce video-level predictions, 20 clips from a video were randomly sampled and presented to each CNN individually and class predictions for each clip were averaged.

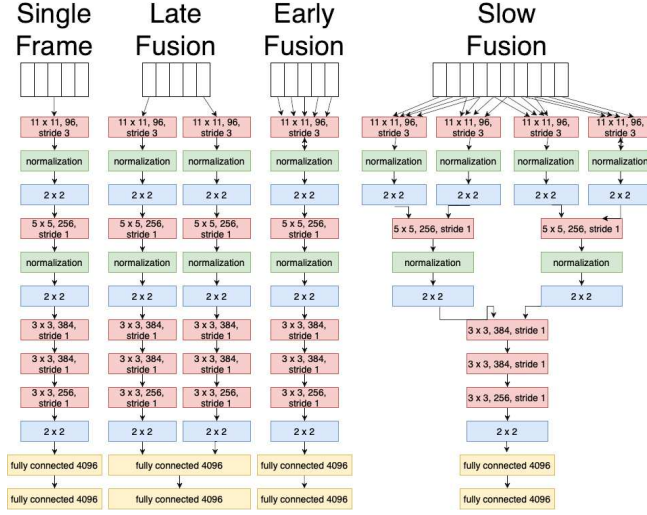


Fig. 5. Approaches [82] tested for fusing information in the temporal domain. Red, green, blue, and yellow layers denote convolution, normalization, pooling, and fully connected layers, respectively. Zoom in to see details. Adapted from [82].

Slow fusion was the best fusion method for video classification on Sports-1M. Interestingly, the single-frame connectivity pattern performed similarly to the other patterns, which showed that learning from a series of frames showed no improvement compared to learning from a static image. The CNN’s learned feature representation trained on Sports-1M was shown to generalize to different action classes and datasets. One transfer learning experiment using UCF101 compared the accuracy of training the CNN from scratch with the accuracies of fine-tuning the top layer, top three layers, and all layers. Fine-tuning the top three layers performed the best, demonstrating that the layers near the top learn dataset-specific features and the lower layers learn more generic features.

Two-stream CNNs [141] capture motion by decomposing videos into a spatial component, which has information about objects and scenes, and a temporal component, which describes the movement of objects and the camera. This approach is based on the two-streams hypothesis from neuroscience [50] which posits that the human visual cortex has a ventral stream that performs object recognition, and a dorsal stream that recognizes motion.

The authors of a new two-stream CNN approach [141] for video classification suggested that features learned through slow fusion in the prior example [82] are not optimal for capturing motion because there is no significant difference between CNN performance on static images, and CNN performance using fusion. In addition, slow fusion was 20% less accurate than the best trajectory-based shallow representation at the time [127]. The team proposed a solution that combined spatial and temporal recognition streams using

late fusion. The temporal stream input is formed by stacking the optical flow displacement fields between a sequence of consecutive frames. Two input configurations were considered. One method does not sample optical flow at the same location across frames, but instead samples the optical flow along the motion trajectories. The other, more successful option, treats the horizontal and vertical components of the optical flow vector field \mathbf{d}_t^x and \mathbf{d}_t^y , respectively, at frame t , as image channels. The optical flow channels of L consecutive frames are stacked to form $2L$ input channels. The CNN input volume $I_\tau \in \mathbb{R}^{w \times h \times 2L}$ for a frame τ is defined as:

$$I_\tau(u, v, 2k-1) = d_{\tau+k-1}^x(u, v), \quad (4)$$

$$I_\tau(u, v, 2k) = d_{\tau+k-1}^y(u, v),$$

where w and h are the width and height of the video, and the displacement vector at point (u, v) in frame t is $\mathbf{d}_t(u, v)$ with $u = [1; w]$ and $v = [1; h]$. The frame and channel indices are $k = [1; L]$ and $c = [1; 2L]$, respectively. The channels $I_\tau(u, v, c)$ represent the horizontal and vertical components of motion of a point (u, v) over L frames. From each displacement field \mathbf{d} , the mean vector is subtracted to perform zero-centering of the network input so that the optical flow between frames is not dominated by a particular displacement caused by camera motion.

This method was evaluated using two datasets: UCF101 and the Human Motion Database (HMDB51) [46]. HMDB51 has 6,766 labeled video clips with 51 classes. The spatial stream CNN was pre-trained on ImageNet. The best performance was recorded when stacking $L = 10$ horizontal and vertical flow fields and using mean subtraction. This method is not end-to-end trainable because a pre-processing step is required to compute optical flow [18] before training. The results established a new state-of-the-art for action recognition.

Even with these improvements, two challenges remained. Two stream approaches developed thus far did not leverage correspondences between spatial cues and temporal cues (optical flow) in videos because fusion is only applied to classification scores. They also had a restricted temporal scale because the temporal CNN operates on a stack of L consecutive optical flow frames. An improved two-stream architecture by Feichtenhofer et al. [41] addresses these issues by fusing spatial and temporal information more effectively across different levels of feature abstraction granularity. For example, the system fuses components like motion (recognized by the temporal network), and location (recognized by the spatial network) to discriminate between actions like brushing teeth and brushing hair. The network is not able to distinguish between these actions when motion or location information is considered separately. The architecture was able to fuse the spatial and temporal networks so that temporal and spatial features correspond (spatial registration). The second limitation is addressed by capturing short-scale optical flow features using the temporal network and putting the features into context over a longer temporal scale at a higher layer.

Fusion functions can be applied at different points in a traditional or two-stream CNN network to implement the fusion approaches we have described. For two feature maps $\mathbf{x}_t^a \in \mathbb{R}^{H \times W \times D}$ and $\mathbf{x}_t^b \in \mathbb{R}^{H' \times W' \times D'}$ at time t , a fusion function $f: \mathbf{x}_t^a, \mathbf{x}_t^b \rightarrow \mathbf{y}_t$ produces an output feature map $\mathbf{y}_t \in \mathbb{R}^{H'' \times W'' \times D''}$, where H , W and D are

the height, width and number of channels. The one constraint is that \mathbf{x}_t^a and \mathbf{x}_t^b have the same spatial dimensions, so we assume $H = H' = H''$, $W = W' = W''$, $D = D'$.

The following functions were proposed to register corresponding pixels in the spatial and temporal stream networks. **Sum fusion** computes the sum of the feature maps at the same spatial locations and channels. **Max fusion** computes the maximum of the feature maps. Concatenation fusion stacks the feature maps at the same spatial locations across different channels using Equation 5, where $\mathbf{y} = \mathbb{R}^{H \times W \times 2D}$. **Convolutional fusion** first stacks the feature maps using concatenation fusion, then convolves the stacked data with a bank of filters $\mathbf{f} \in \mathbb{R}^{1 \times 1 \times 2D \times D}$ accounting for biases $\mathbf{b} \in \mathbb{R}^D$. When used as a trainable filter kernel, \mathbf{f} learns correspondences of feature maps that minimize a joint loss function. We include the formulation for convolutional fusion in Equation 6 (with the intermediate concatenation step Equation 5) as it has been found to be the most effective of these fusion methods.

$$\mathbf{y}_{i,j,2d}^{cat} = \mathbf{x}_{i,j,d}^a \mathbf{y}_{i,j,2d-1}^{cat} = \mathbf{x}_{i,j,d}^b \quad (5)$$

$$\mathbf{y}^{conv} = \mathbf{y}^{cat} * \mathbf{f} + \mathbf{b}. \quad (6)$$

Bilinear fusion computes a matrix outer product of the feature maps at each pixel, then performs a summation over the pixels. The result captures multiplicative interactions between pixels in a high dimensional space. For this reason, in practice, bilinear fusion is applied after the fifth ReLU activation function and fully connected layers are removed. Ultimately each channel of the spatial network is combined multiplicatively with each channel of the temporal network.

As previously mentioned, convolution fusion was the best approach. When evaluating this fusion method, it was determined that additional computation speed-ups could be achieved by first combining feature maps over time using pooling methods before convolving with the filter bank. This effectively reduced the parameter space by reducing the feature map size. Two pooling scenarios were considered. Network predictions were averaged over time (2D pooling), or max pooling was applied to stacked data in a 3D cube (3D pooling). Three-dimensional pooling increased performance more than 2D pooling. The network was fused spatially and truncated after the fourth convolutional layer to find a balance between maximizing classification accuracy and minimizing the total number of parameters. The fused architecture showed improvement upon previous state-of-the-art action recognition methods [141, 156] on UCF101 and HMDB51.

Another challenge with two-stream approaches developed thus far, is the increased time and storage requirements due to their reliance on pre-computed optical flow before CNN training [141]. MotionNet [180] introduced new time and storage efficiencies with a CNN that produced optical flow from video clips on-the-fly. The results were similar to the optical flow generated by one of the best traditional methods [174]. Optical flow estimation was framed as an image reconstruction problem. Using two consecutive frames I_1 and I_2 as input, MotionNet generated a flow field \mathbf{V} which was used with I_2 to create a reconstructed frame I_1' using the inverse warping function [68].

MotionNet aims to minimize the photometric error between I_1 and I_1' . Assuming I_1 and I_1' are related by a parametric transformation, the minimization function finds the parameters of the transformation \mathbf{p} that minimize the squared intensity error:

$$\operatorname{argmin}_{\mathbf{p}} \sum_{\mathbf{u} \in \alpha_1} \frac{1}{2} \|I_1(\mathbf{u}) - I_1'(w(\mathbf{u}; \mathbf{p}))\|^2 \quad (7)$$

where $\mathbf{u} \in \alpha_1$ is a subset of pixel coordinates in image I_1 and w is the warping function [7]. Traditionally the Lucas-Kanade algorithm [7, 102] solves Equation 7 and is used to calculate optical flow. MotionNet produces optical flow using three novel unsupervised loss functions which we describe below.

A **pixelwise reconstruction error function** is used to measure the difference in pixel values between the frames:

$$L_{pixel} = \frac{1}{hw} \sum_i^h \sum_j^w \rho(I_1(i, j) - I_2(i + V_{i,j}^x, j + V_{i,j}^y)) \quad (8)$$

where h and w are the height and width of images I_1 and I_2 . The horizontal and vertical components of the estimated optical flow are denoted as V^x and V^y . The term $\rho(x) = (x^2 + \epsilon^2)^\alpha$ denotes the generalized Charbonnier loss function which is a differentiable version of the L_1 norm used to decrease the influence of outliers, where ϵ determines how closely it resembles the L_1 norm. The arbitrary power α is non-convex when $\alpha < 0.5$.

A **smoothness loss function** resolves ambiguities that occur when estimating motion in non-textured local regions (aperture problem). It is difficult to detect motion on local image patches using convolution if patches are not textured. Let ∇V_x^y and ∇V_y^y be the gradients of the vertical component of the estimated flow field, and ∇V_x^x and ∇V_y^x be the gradients of the horizontal component. Smoothness loss is defined as:

$$L_{smooth} = \rho(\nabla V_x^x) + \rho(\nabla V_y^x) + \rho(\nabla V_x^y) + \rho(\nabla V_y^y) \quad (9)$$

The **structural similarity loss function** helps the network learn frame structure. A sliding window approach is used to partition I_1 and I_1' into local patches for comparison. Let N denote the number of patches that can be extracted from the image using a sliding window with stride 8, let n denote the patch index, and let I_{1n} and I_{1n}' denote two image patches from the original image I_1 and its reconstruction I_1' :

$$L_{ssim} = \frac{1}{N} \sum_n^N (1 - SSIM(I_{1n}, I_{1n}')), \quad (10)$$

where SSIM measures the perceptual quality of frames computed as:

$$SSIM(I_{p1}, I_{p2}) = \frac{(2\mu_{p1}\mu_{p2} + c_1)(2\sigma_{p1p2} + c_2)}{(\mu_{p1}^2 + \mu_{p2}^2 + c_1)(\sigma_{p1}^2 + \sigma_{p2}^2 + c_2)}. \quad (11)$$

SSIM determines the average dissimilarity between images by examining the means μ_{p1} and μ_{p2} , variances σ_{p1} and σ_{p2} , and covariance σ_{p1p2} of the pairs of image patches. Two constants c_1 , and c_2 are used to stabilize the division.

Loss was computed at each scale s as a weighted sum of the three loss functions, where λ_1 , λ_2 , and λ_3 weigh the importance of each loss function:

$$L_s = \lambda_1 L_{pixel} + \lambda_2 L_{smooth} + \lambda_3 L_{ssim} \quad (12)$$

MotionNet was combined with a temporal stream CNN which learned to map the generated optical flow to class labels for action recognition. Two methods for combining models were explored. Stacking simply concatenated the two networks with MotionNet placed in front. Branching used a single network for optical flow extraction and action classification, and then shared features between the two tasks. Stacking proved more space efficient than branching. Multiple strategies were explored for fine-tuning the stacked CNN for action recognition. The strategy with the highest performance fine-tuned both networks (MotionNet and the temporal CNN) utilizing all three loss functions. Long-term motion dependencies were represented using a sequence of 11 frames which yielded multiple (10) optical flow fields.

The proposed method [180] outperformed real-time action recognition methods at the time ([37, 80, 119, 156, 169, 175]) on four benchmarks datasets; UCF101, HMDB51, THUMOS14 [75], and ActivityNet [59]. THUMOS14 and ActivityNet are large datasets of long, untrimmed videos. MotionNet was shown to be flexible as it may be concatenated to deeper CNN architectures to improve their recognition accuracy. Such frameworks are still real-time due to the on-the-fly optical flow calculation.

3D CNNs use spatio-temporal convolutions that model both spatial structure and temporal information in sequences. They operate on the premise that 3D convolutions preserve temporal information from input signals while 2D convolutions collapse temporal information.

C3D [156] is a 3D CNN that achieved a new state-of-the-art in object recognition and scene classification in videos. The approach found that the homogenous setting of $3 \times 3 \times 3$ kernels in all convolutional layers is the best option for 3D CNNs which is consistent with VGGNet (Figure 6, right). The architecture has 8 convolutional layers with $3 \times 3 \times 3$ convolutional filters, 5 max pooling layers and 2 fully connected layers followed by a softmax output layer. Pooling layers are $2 \times 2 \times 2$, except for the first layer which is $1 \times 2 \times 2$ to help preserve temporal information. The stride is 1 for pooling and convolution. Video clips each consisting of 16 frames were the network inputs. The architecture was designed to be as deep as possible while accounting for training on a large dataset, GPU memory, and computation affordability.

The C3D network is trained from scratch on the Sports-1M dataset. The trained network was used as a feature extractor for different tasks including action recognition on UCF-101, action similarity labeling, scene and object recognition. The learned features were evaluated for action recognition and showed 5% improvement compared to slow fusion [82]. Evaluation on UCF101 produced an 11% improvement over the slow fusion model [82] for action recognition.

Three-dimensional CNNs like C3D have several advantages. The performance of C3D was similar to the original two-stream approach [141], but with a lower runtime. C3D does not use optical flow as

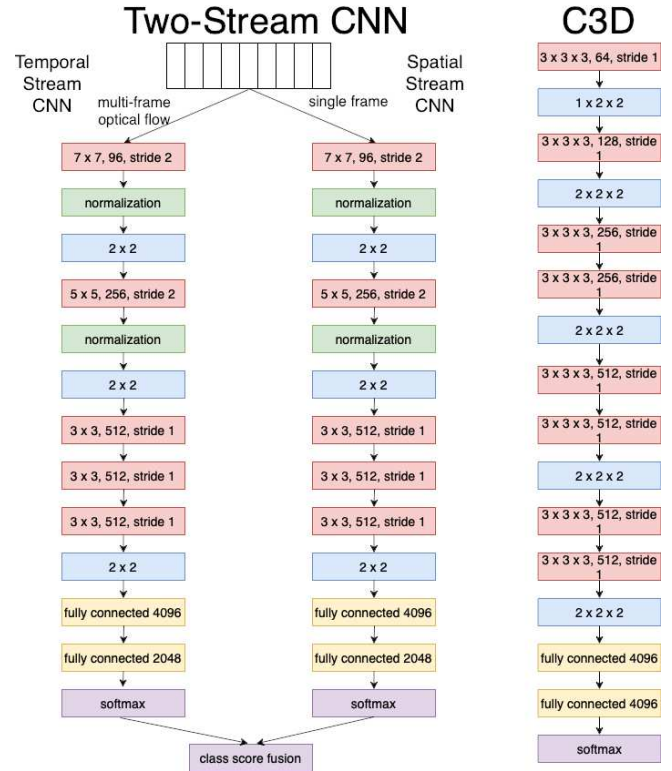


Fig. 6. Two-Stream Video Classification Architecture (left) [141] and C3D Architecture (right) [156]. Red, green, blue, and yellow layers denote convolution, normalization, pooling, and fully connected layers, respectively. Zoom in to see details. Adapted from [141] and [156].

input like the two-stream architecture [141] does, and instead extracts motion features directly from videos. There are still some drawbacks. Three-dimensional CNNs are harder to train than 2D CNNs because they have many more parameters from the extra filter dimension. In addition, C3D did not benefit from performance improvements from ImageNet pre-training [36] because it is a relatively shallow architecture trained from scratch.

A novel two-stream *Inflated* [83] 3D CNN, I3D [24], improved upon the previous state-of-the-art in action recognition [41, 141, 156] by inflating 2D CNN image classification models into 3D CNNs. This inflation process adds a temporal dimension to the filters and pooling kernels in a 2D CNN.

Transfer Learning on Video Datasets: Originally, it was unclear whether transfer learning was as useful for videos. A new dataset, the Kinetics-400 Human Action Video Dataset [83], was collected to evaluate this. This dataset contains about 306,245 videos that correspond to 400 human action classes, with over 400 clips for each class. The dataset is split into training, test and validation sets. Several architectures including the original two-stream approach [141], C3D [156], the 3D fused two-stream approach [41], and I3D [24], were compared by first pre-training on the Kinetics-400 dataset, then fine-tuning on HMDB51 and UCF101. The difference between the performances of the best deep network, I3D [24],

and the best hand-crafted approach, iDT [168], for video action recognition was smaller than the difference between that of the best deep learning-based and hand-crafted image recognition approaches. Additionally, a 2D CNN applied to individual frames of a video performed comparably to I3D on the Sports-1M dataset. This work [24] demonstrated that there is considerable benefit to transfer learning in videos. Kinetics-600 [23], the second iteration of the Kinetics dataset contains about 500,000 10-second long videos sourced from YouTube that correspond to 600 classes.

The aforementioned transfer learning results inspired a subsequent work [157] that reconsidered 3D CNNs in the context of residual learning. ResNets use skip connections to speed up network learning and permit substantially deeper networks that can learn more complex functions. 3D ResNets have additional dimensions, 3D convolutions and 3D pooling. Three-dimensional ResNets outperformed 2D ResNets in action recognition. The team also investigated several forms of spatio-temporal convolution: 2D convolution on frames, 2D convolution on clips, 3D convolution, 2D-3D convolution, and a factorization of 3D convolution into 2D spatial convolution followed by 1D temporal convolution ($R(2+1)D$ convolution). Using $R(2+1)D$ convolution doubled the number of nonlinearities in the network. This facilitated gradient optimization and enabled more complex function representations. During evaluation experiments, the $R(2+1)D$ convolutional block achieved state-of-the-art accuracy on the Kinetics-400 and Sports-1M datasets. The team also investigated whether the model supported transfer learning by pre-training on Kinetics-400 and Sports-1M and then fine-tuning on UCF101 and HMDB51. In the transfer learning experiment $R(2+1)D$ outperformed all other methods except for I3D, which uses Kinetics-400 and ImageNet for pre-training. Table 5 summarizes the action recognition approaches discussed in this section, and their performance on UCF101.

Improving Computational Cost of 3D CNNs: MF-Net uses an ensemble of lightweight networks (fibers) instead of one complex network to improve performance while reducing computation cost. The 3D Multi-Fiber architecture was designed for human action recognition and achieved better accuracy on Kinetics-400, UCF101, and HMDB51 compared to other 3D CNNs like I3D [24] and $R(2+1)D$ [157] while using fewer FLOPs.

5 ANIMAL BEHAVIOR CLASSIFICATION

This section reviews adaptations of the learning models presented in Sections 3 and 4 for animal behavior classification. We focus on models that analyze small laboratory animals in neuroscience. Figure 1 gives a graphical overview of the classification frameworks, pose estimation and tracking methods organized by the CNN networks they use. Figure 4 shows the relationship of several animal classification approaches to spatio-temporal infrastructures for human action recognition. Figure 7 shows the relationship of techniques reviewed in this section to human action recognition and human pose estimation methods. We include systems that are significantly different so that important developments in the underlying deep learning architectures are represented. We also indicate validation animal types, social interaction support, and whether depth

cameras are required. Optical flow methods are identified. Human pose estimation taxonomy categories [177] (Section 3) are shown.

We begin with background information on manual scoring for labeling videos, with a brief overview of the challenges with traditional vision approaches that lead to breakthroughs in deep learning-based classification solutions. In Sections 5.1 and 5.2, we review animal pose estimation as many frameworks require a pose estimation before presenting our taxonomy for organizing these frameworks in Section 5.4.

Manual Behavior Scoring: Quantification of animal behavior is important in ethology and behavioral neuroscience [55]. However, it is well known that manual scoring of animal behavior videos is time-intensive, costly, and subjective [55]. Subtle fine-level behaviors may go undetected as behaviors must be pre-defined [135]. Manual behavioral scoring is also subject to human bias as results can vary between different research labs and between researchers within the same lab [14, 55, 139]. Moreover, individual scorers themselves may drift over time as they gain experience [86]. Thus, scoring by the same individual may change across different sessions.

Traditional Methods use automated software to facilitate manual behavior scoring. There are several challenges with the application of these methods across research labs. Early automated methods often relied on specialized equipment like depth cameras [172] which may be costly or require expertise to operate. Some methods require that markers are placed on animals [108] for motion tracking. The use of markers is less desirable because they can be intrusive, and their locations must be determined a priori. Markers can also distract the animal in a way that alters its behavior and skews experimental results. It is common for traditional systems to use older computer vision processing techniques [34] without incorporating neural networks. These methods require supervision in the form of pre-selected labels specified by the researcher. They also require highly controlled laboratory environments and have limited ability to track multiple animals. Commercial software and other solutions that do not offer publicly available open-source code are harder to reuse and adapt for different experiments.

The Promise of Deep Learning Solutions: Deep learning methods are better suited for these problems [54, 116] as they permit multiple unmarked animals to be tracked in almost any context, including in-the-wild. These techniques are widely applicable because they generally operate using RGB cameras and are often developed as open-source platforms. Some open-source solutions outperform commercial software with added flexibility for customization which can facilitate adoption. Pose-based approaches are relatively subjective and may not generalize across labs and experiments if animals vary in size or camera frame rates are different [61]. Approaches that classify behavior directly from raw pixel values without estimating pose mitigate this issue and simplify the behavior classification pipeline [14]. Data dependent factors make systems difficult to generalize pipelines (frame-rate, intensities) [10]. We now review several deep learning algorithms that have led to advancements in behavior analysis in neuroscience.

5.1 2D Animal Pose Estimation

This section reviews CNN network architectures for 2D animal pose estimation that leverage methods discussed in Sections 3 and 4. We cover 3D techniques in the next section. Table 8 summarizes the key contributions of 2D and 3D animal pose estimation methods, indicating validation animal types, method type, and the number of cameras required. Coarse level supervision is indicated (pink: supervised, blue: unsupervised). Common animal behavior video datasets are found in Table 6.

An early deep learning-based approach for 2D animal pose [172] classified sub-second structure in mice behavior using unsupervised learning. The approach first compressed videos of freely moving mice using principal component analysis (PCA). It then used an auto regressive hidden Markov model to segment the compressed representation into discrete behavioral syllables, identifiable modules (like grooming and rearing) whose sequence is governed by definable transition statistics. The technique requires special depth cameras. These are limiting because they may not detect very small laboratory animals and reconstructing full 3D poses is challenging without multiple camera viewpoints.

DeepLabCut [108] was the first tool to extend human pose estimation techniques to the animal pose estimation problem [109]. The approach modified the feature detector architecture in DeeperCut [66] which builds upon ResNet (Section 3.1 and Figure 1). The toolkit tracks multiple animals' 3D poses in 2D images. Camera calibration with one or more cameras is used to find 3D keypoint locations. DeepLabCut requires 200 labeled frames because it uses a model pretrained on ImageNet. Multi-animal DeepLabCut [90] extends DeepLabCut to the multi-animal setting. The authors achieve this by adopting aspects of three CNN architectures [22, 58, 150] and using a transformer [95, 181] architecture to reidentify animals when they leave the field of view.

LEAP [128] was designed to estimate poses in videos of individual mice and fruit flies. It adapts three CNNs originally developed for human pose estimation [118, 154, 170] into a fully convolutional architecture that predicts heat-maps for body parts from frames. The solution uses an active learning (Section 2) approach that requires at least 10 labeled frames. Two-dimensional pose is estimated at each time step. A spectrogram is computed for the time-series of each joint using a continuous wavelet transform. Spectrograms are then concatenated and embedded in a 2D manifold (behavior space) where each video is represented as a feature vector that captures 2D pose dynamics across time. The behavior space distribution is then clustered to identify classes of behaviors. The complete pipeline from pose estimation to behavioral clustering for behavior recognition is semi-supervised. The output of LEAP was used for unsupervised analysis of the fly behavior repertoire.

SLEAP (Social LEAP) [129], the successor to LEAP, is a general framework for multi-animal pose estimation. It implements bottom-up and top-down pipelines, identity tracking using motion and appearance models, and over 30 neural network architectures. Our graphical overview (Figure 1) uses the default architecture used in SLEAP, a version of UNet [136]. UNet is an encoder-decoder architecture designed for segmentation of biomedical images. SLEAP

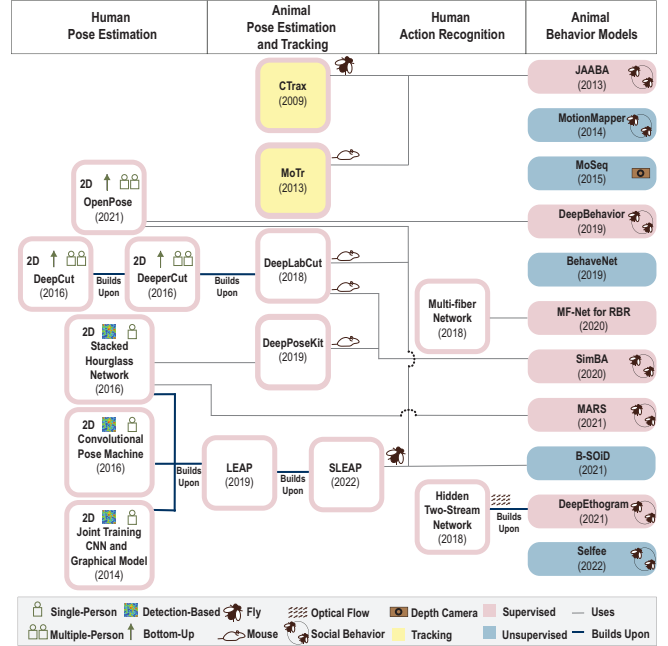


Fig. 7. Animal Behavior Classification Frameworks and the Action Recognition, Pose Estimation and Tracking Methods they Use or Build Upon.

Dataset	Year	Trimmed	Size	Social	Classes
Clipped Mouse [72]	2010	✓	4, 268	✗	8
Full Mouse [72]	2010	✗	12	✗	8
CRIM13 [20]	2012	✗	474	✓	13
Sturman – EPM [146]	2020	✗	24	✗	6
Sturman – FST [146]	2020	✗	29	✗	2
Sturman – OFT [146]	2020	✗	20	✗	4
Mouse Ventral1 [14]	2021	✗	14	✗	28
Mouse Ventral2 [14]	2021	✗	14	✗	16
Mouse OpenField [14]	2021	✗	20	✗	6
Mouse – HomeCage [14]	2021	✗	11	✗	8
Mouse – Social [14]	2021	✗	12	✓	6
Fly [14]	2021	✗	19	✗	2

Table 6. Common Animal Behavior Video Datasets

is designed to be flexible to allow the comparison of part grouping approaches, identity tracking approaches, and neural network

architecture properties. SLEAP achieves comparable or improved accuracy when compared to DeepPoseKit, LEAP, and DeepLabCut for single-animal pose estimation with faster inference speed.

DeepPoseKit [54] is a single-animal 2D pose estimation method. The project evaluates two models: a new stacked DenseNet CNN [71] network, and a modified stacked hourglass network [118] that has origins in human pose estimation. In DenseNets [64], each layer is connected to every other layer in a feed-forward fashion to mitigate the vanishing gradient problem and decrease parameterization. The stacked hourglass architecture [118] is an encoder-decoder network with several pooling and upsampling layers. Each hourglass module processes features to a low resolution then upscales and combines the features from multiple scales. This design captures information at every scale and allows intermediate supervision. Of the two methods, the stacked DenseNet was found to perform better.

Previous pose estimation methods like DeepLabCut have not been effective in tracking multiple identical animals. AlphaTracker [29] is a recently developed tool for multiple-animal tracking that adapts a human pose estimation algorithm, AlphaPose, for animal pose estimation. The positions of animals in each frame are detected using YOLOv3 [134]. The resulting bounding boxes are cropped and fed to a Squeeze-and-Excitation network (SE-Net) [62] to estimate pose, and the identities of mice are tracked across frames. Squeeze-and-Excitation (SE) networks [62] use SE blocks to improve a CNNs representational capacity by explicitly modeling the interdependencies between convolutional feature channels. Training requires labels, though features extracted from the keypoints are clustered into individual or social behaviors using hierarchical clustering in an unsupervised manner. Calibration is automated.

Speed Accuracy Trade-Off When choosing a pose estimation architecture, the speed-accuracy trade-off must be considered [65]. DeepLabCut prioritizes accuracy over speed by using a large overparameterized model (ResNet). This overparameterization leads to relatively slow inference but maintains accurate predictions. The LEAP system [128] prioritizes speed by using a smaller less-robust model. Although it has a faster inference time, it is less robust to data variance and less likely to generalize to different environments. DeepPoseKit aims to improve processing speed without sacrificing accuracy, and reports that the approach is about three times as accurate as LEAP, as accurate as DeepLabCut [108], and twice as fast as both (Table 7).

Approach	Mean Accuracy	Inference Speed (Hz)
DeepLabCut [108]	0.33	520
LEAP [128]	0.13	560
DeepPoseKit [54]	0.35	1000

Table 7. Inference Speed and Posterior Mean Accuracy for 2D Animal Pose Estimation Approaches. Data sourced from [54].

5.2 3D Animal Pose Estimation

A two-dimensional pose is an incomplete representation of an animal’s behavior as occlusions (that hide limbs) result in loss of important information. Camera viewing parameters also affect how movement is quantified. DeepLabCut used a printed checkerboard target to calibrate cameras for 3D pose estimation. This type of target would not work well for analyzing small animals like flies (the *Drosophila melanogaster* fly is 2.5 mm long). Calibration patterns would have to be extremely small, and color would introduce imaging artifacts at translucent body parts. DeepFly3D [56] adapted the stacked hourglass network architecture [118] and added tools to compute the accurate 3D pose of *Drosophila melanogaster* using the fly itself as the camera calibration target. Although the approach can be used for any animal type or species, it requires multiple camera views. Like LEAP, 2D pose data and 3D joint angles are used for unsupervised behavioral classification by clustering after 3D pose estimation. When the two data sources were compared, classification using 3D joint angles resulted in clearer clusters of behaviors. LiftPose3D [52] only requires one camera view, a prism mirror, and 1,000 – 10,000 training images. The approach is based on a CNN architecture developed for mapping 2D human poses to 3D poses using a single camera view [107] (Section 3). Another method, AniPose [81], built on DeepLabCut, allows 3D reconstruction from multiple cameras using a wider variety of methods.

MouseVenue3D [57] contributed an automated 3D behavioral capture system that uses multi-view cameras to estimate 3D pose in marker-less rodents. This work showed that 3D behavioral data yields improved performance in behavior recognition tasks compared to 2D behavioral data.

5.3 Tracking

Here, we review two tracking methods used by the animal behavior classification frameworks we discuss.

CTrax [15] is a computer vision system designed to identify the position and orientation of multiple flies in a 2D arena in each frame of input videos. Flies are detected first through background subtraction and then fitting an ellipse to each fly by fitting a Gaussian to each fly’s pixel locations. Next, flies are assigned identities using the Hungarian algorithm for minimum-weight perfect bipartite matching.

MoTr (Mouse Tracker) [123] is a computer vision system similar to CTrax [15] designed for tracking multiple mice in a 2D arena. Flies are detected through background subtraction and fitting ellipses to mice using the expectation-maximization algorithm. Then a hidden Markov model is used to associate mouse identities with trajectories. Multiple mice are recognized in overhead videos by applying distinct patterns to the back of each mouse and training a classifier on histogram of oriented gradients (HOG) [158] features extracted from image patches containing individual mice.

5.4 Taxonomy for Animal Behavior Classification

This section provides a high-level overview of animal behavior classification frameworks for small laboratory animals. We outline a general taxonomy that organizes methods as supervised or unsupervised at a coarse level, and with varying degrees of supervision

Taxonomy for Animal Behavior Classification	
Supervised Classification	
Hand-crafted Features, Behavior Labels	[137], [33], [72], [20], [47], [79], [60], [101], [35], [45]
Behavior Labels	[91], [160], [63]
Hand-crafted Features, Pose and Behavior Labels, PE	[139], [145], [146], [4], [94], [121]
Pose and Behavior Labels, PE	[179]
Optical Flow, Hand-crafted Features, Behavior Labels	[161]
Residual Learning, Optical Flow, Behavior Labels	[14]
Residual Learning, Pose and Behavior Labels, PE	[178]
Residual Learning, Optical Flow, Behavior Labels	[105]
Unsupervised Classification	
Hand-crafted Features, Pose Labels, PE	[61]
Fully Unsupervised	[144], [11], [172], [8], [16], [73]

Fig. 8. Taxonomy for Animal Behavior Classification. Pink: supervised, Blue: unsupervised

influenced by inputs, framework components and learning strategies. Supervised methods require manual labels for classification while unsupervised methods automatically cluster the data and assign labels. Within these groups we consider the influence of hand-crafted features, labels (Pose or Behavior), pose estimation (PE), optical flow, and residual learning. We focus on optical flow and residual learning as a study [120] showed improvement when using 3D CNNs pre-trained to recognize human behaviors, then fine-tuned on mouse behavior datasets. This study used two-stream fusion with I3D and R(2+1)D by calculating optical flow on a dataset of solitary mice videos [72]. R(2+1)D uses residual learning. Table 9 summarizes key contributions of these frameworks with coarse level of supervision indicated (pink: supervised, blue: unsupervised). The table also indicates whether pose estimation or depth cameras are required, the type of animal used for validation, and whether there is support for individual or social interactions. Figures 9, 10 and 11 diagram a representative set of systems (posed-based, supervised without pose estimation, and unsupervised without pose estimation respectively).

Supervised Classification requires behavior labels.

- **Hand-crafted Features, Behavior Labels:** These examples use computer vision processing methods to fit shapes (ellipses) to the animal body, extract features, and apply neural networks to classify learned features to behaviors.
 - One of the first works to apply neural networks to animal behavior analysis [137] trained a three-layer feed-forward neural network on 3 parameters that describe a rat’s position, achieving a 63% accuracy over nine behaviors.
 - Caltech Automated Drosophila Aggression-Courtship Behavioral Repertoire Analysis (CADABRA) [33] measured social behaviors from overhead videos of fly pairs. Fly bodies were localized [12], and fitted with ellipses before calculating features (size, position and velocity). K-nearest-neighbors was used to classify actions from the features.

- A later study [72] extracted per-frame features of a rodent and used a SVM hidden Markov model (SVMHMM) [1] to output behavioral labels. The primary dataset was a single black mouse with a white background. A dataset with per-frame labels of eight solitary behaviors of a mouse in a standard enclosure over ten hours was also released.
- The next development [20] focused on social interaction between two mice with unconstrained colors. The algorithm tracks rodents, calculates features, and applies AdaBoost to classify trajectory and spatiotemporal context features. The Caltech Resident-Intruder Mouse (CRIM13) dataset [20] was released with 13 action classes and 237 10-minute videos (8 million frames, over 88 hours) of top and side views of mice pairs engaging in social behavior. A 2013 study [47] generalized this framework to support more mice and different experimental settings using a temporal random forest classifier.
- Janelia Automatic Animal Behavior Annotator (JAABA) system [79] (Figure 10) fits ellipses to body outlines using CTrax (Section 5.3), and then calculates per-frame features from the trajectory. A Gentleboost algorithm [43] classifies behaviors using per-frame *window* features and manually collected behavior labels.
- Later Hong et. al. [60] trained a random forest classifier on location, appearance, and movement features extracted from egocentric depth maps, and five learned pose parameters to identify social rodent behaviors. A social behavior analysis project [101] used GMM and EM algorithms (like CTrax) to track features.
- LiveMouseTracker [35] is a method for real-time tracking of rodent trajectories for behavior analysis of up to four mice. An infrared-depth camera segments and removes the background from frames, and a random forest algorithm identifies rodents and their orientations (shape and posture) from labels. Individual and social behavioral traits were extracted.

- DEcoding Behavior Based on Positional Tracking (BehaviorDEPOT) [45] is a software program for behavior recognition in videos. It uses heuristics to measure human-defined behaviors from pose estimation data (from DeepLabCut) that are easier to interpret than traditional supervised machine learning methods.
- **Behavior Labels:** These approaches use labels but avoid hand-crafted features as they must be defined a priori and may not generalize to different behaviors [63].
 - A 3D CNN [91] similar to C3D was used to extract short-term spatio-temporal features from clips. These features are fed to an RNN with LSTM blocks to produce long-term features. A SoftMax layer outputs the probabilities of behaviors in each clip. This approach slightly underperformed when compared to an approach that used handcrafted features [72].
 - A multi-fiber neural network (MF-Net) [27, 160] (Figure 10) has been used to classify videos for rat behavior recognition (RBR). The architecture has one 3D convolutional layer followed by four multifiber convolutional blocks. Results outperformed the prior work of this team [161] when tested on the same dataset (see discussion of EthoVision XT RBR). However, MF-Net uses data augmentation which did not generalize to different set-ups or animals. Note one less successful option in the paper used optical flow.
 - The LabGym [63] framework provides customizable combinations of neural networks to assess spatiotemporal information in videos. It runs easily on a common laptop, without the need for powerful GPUs required by DeepEthogram [14] and SIPEC [105] (which we describe later). It is not optimized for social behavior analysis but is effective for invertebrate and mammal behavior analysis.
 - **Hand-crafted Features, Pose and Behavior Labels, PE:**
 - The Mouse Action Recognition System (MARS) [139] (Figure 9) focuses on social behaviors between a black and white mouse. It adapts a stacked hourglass architecture (Section 5.1) with eight hourglass subunits to estimate pose. The rolling feature-window method from JAABA is used to calculate handcrafted features over a time window. XGBoost [25] is trained to predict behaviors given the window features.
 - The DeepBehavior toolbox [4] (Figure 9) uses a version of GoogLeNet [145] or OpenPose [22] (depending on the species) for kinematic analysis of three rodent behaviors in 3D. Stewart and colleagues designed an architecture [145] for multiple object detection using GoogLeNet to encode images into high level descriptors before decoding the representation into a set of bounding boxes using an LSTM layer. Experiments were conducted using one or two cameras.
 - Simple Behavior Analysis (SimBA) [121] (Figure 9) classifies behaviors based on the locations of certain key points, or joint locations, obtained from 2D pose estimation methods (like DeepLabCut, LEAP and DeepPoseKit). After detecting poses, outliers are identified and corrected. There are 498 metrics calculated from corrected pose data over rolling windows (like JAABA). Random forest classifiers are trained to predict behavior classes given the calculated features. In a related approach [146], DeepLabCut is used for per-frame pose estimation, before applying a feedforward neural network to classify pose features as behaviors. Sturman et al. [146] released three video datasets of mice behavioral tests, including the open field test (OFT), elevated plus maze (EPM), and forced swim test (FST).
 - OpenLabCluster [94] contributed unsupervised clustering (Section 2) of pose features using a deep recurrent encoder-decoder architecture and an active learning approach (Section 2). In the latter approach, at each iteration, one sample is labeled, and the cluster map is refined. A fully-connected network is appended to the encoder to perform classification trained on labeled samples. The results produce fast and accurate classification in four animal behavior datasets with sparse labels.
- **Pose and Behavior Labels, PE:**
 - ContrastivePose [179] uses contrastive learning to reduce differences in pose estimation features and its random augmented version, while increasing differences with other examples. These features have a similar structure as handcrafted features and perform comparably on semi-supervised behavior classification.
 - **Optical Flow, Hand-crafted Features, Behavior Labels:**
 - The EthoVision XT RBR [122, 161] is commercial software that tracks features using optical flow estimated with the Lucas-Kanade algorithm [7, 102]. Features are reduced to a low-dimensional space using the Fisher linear discriminant analysis [44] before applying a quadratic discriminant for classification. The testing dataset (solitary rats with per-frame labels of 13 behaviors) is not public.
 - **Residual Learning, Optical Flow, Behavior Labels:**
 - DeepEthogram [14] (Figure 10) generates an ethogram (a set of user defined behaviors of interest). The system builds upon a two-stream approach that computes optical flow on the fly. First the flow generator is trained on unlabeled videos, while the user labels each frame of some videos in parallel. ResNet models extract per-frame flow and spatial features. A CNN with Temporal Gaussian Mixture (TGM) layers [132] learns a latent hierarchy of sub-event intervals from untrimmed videos for temporal action detection. The TGM has a large temporal receptive field, and outputs the final probabilities that indicate whether the behavior exists at each frame. Thus, this method integrates aspects of

action detection methods (Section 1.1) as information from seconds ago helps classify current behaviors. Five benchmark datasets of mice in different arenas were released, including one with social interaction, and one with flies to test if the system generalized to other species.

- **Residual Learning, Pose and Behavior Labels, PE:**

- A recent work [178] models interactions between mice using a Cross-Skeleton Interaction Graph Aggregation Network (CS-IGANet). A Cross-Skeleton Node-level Interaction (CS-NLI) models multi-level interactions between mice and fuses multi-order features. An Interaction-Aware Transformer for the dynamic graph updates, and node-level representations, was proposed. DeepLabCut is used to estimate pose for datasets without pose labels. A self-supervised task for measuring the similarity of cross-skeleton nodes was also proposed. This approach outperforms other approaches on the CRIM13 dataset.

- **Residual Learning, Optical Flow, Behavior Labels:**

- Segmentation, Identification, Pose-Estimation and Classification (SIPEC) [105] contributed multiple deep neural network architectures for individual and social animal behavior analysis in complex environments. These networks operate on pixels. SegNet [6] is a well-known CNN architecture for pixel-wise segmentation of images on which SIPEC:SegNet is built. SIPEC:IdNet uses DenseNet to produce visual features that are integrated over time through a gated recurrent unit network [31] to reidentify animals when they enter or exit the scene. SIPEC:PoseNet performs top-down multi-animal pose estimation. SIPEC:BehaveNet uses an Xception network [30] and a Temporal Convolution Network [162] to classify behaviors from raw pixels. This system was the first to classify social behaviors in primates without pose estimation. Note that the classification pipeline (which is our focus) is not pose-based.

Unsupervised Classification: These methods do not require behavior labels for the classification step. The learning process may require input from a supervised pose estimation system (that requires labels). However, the final classification is determined by an automated process that generates and assigns labels (like numeric values) to the output of a clustering system.

- **Hand-crafted Features, Pose Labels, PE:**

- Behavioral Segmentation of Open-field in DeepLabCut (B-SoiD) [61] (Figure 9), uses DeepLabCut (Section 5.1), to obtain six joint locations (snout, four paws, tail base) per frame, then calculates spatiotemporal relationships (speed, angular change, and distance between joints). Features (like speed) are projected from a High-dimensional space to a low-dimensional space using UMAP [111]. HDBScan [21] clusters the results, and a random forest classifier is trained

to predict behaviors directly from high-dimensional features without the computationally expensive clustering step. The need to evaluate and transfer non-linearities from dimensionality reduction is also avoided.

- **Fully Unsupervised:**

- PCA has been applied to a worm’s centerline (which describes most of a worm’s behavior) to represent the *eigenworm* [144] as three values. Unsupervised learning has been used to detect behaviors as sequences of eigenworm positions [17], before clustering using affinity propagation [42].
- MotionMapper [11] (Figure 11) classifies fruit fly behaviors. The system shows that fruit fly posture can be captured by a low dimensional subspace of eigenmodes. PCA analysis projects a processed (segmented, resized and aligned) frame (to a set of 50-dimensional time-series. A Morlet wavelet transform [53] is then applied to create a spectrogram for each postural mode. The wavelet’s multi-resolution time-frequency trade-off reflects postural dynamics at different time scales. Then, t-SNE [163] is used to embed the spectrograms to a 2D space and preserve the local structure of clusters. Finally, a watershed transform [113] segments the embedding and identifies individual behavior peaks. In a related approach [165], a type of hierarchical clustering is used to describe the behaviors of *Drosophila* larvae. This experiment characterized behavior through the identification of 29 atomic movements and four movement categories. MotionMapper [85] was later extended to classify paired fruit-fly behaviors by first segmenting the two flies in each frame.
- Motion Sequencing (MoSeq) [171, 172], (Figure 11), embeds a depth video of an animal into a ten-dimensional space using PCA. An AR-HMM is then fit to the principal components to generate behavioral syllables, producing a dynamical and behavioral representation. The need for a parameter that controls the time scale of transitions between behavioral states can be eliminated by finding motifs of varied lengths [17] or using time-frequency analysis like a wavelet transform [11, 85]. Wavelet transforms can capture multi-scale postural dynamics.
- BehaveNet [8] (Figure 11) builds upon MoSeq [172]. It uses convolutional autoencoders (CAEs) instead of PCA to generate a low-dimensional continuous representation of behavior. An AR-HMM is used to segment the representation into behavioral syllables.
- Unsupervised behavior analysis and magnification (uBAM) [16] introduces a neural network designed to compare behaviors, and another designed to magnify differences in behavior. This allows classification behavior extraction and analysis of small behavioral differences, without using any pose or behavior labels.

Method	Year	Multiple Animals	Validated	2D/3D	Multiple Cameras	Key Contribution(s)
DeepLabCut [108]	2018	✗	Mice, Flies, Humans, Horses, Fish	2D/3D	✓	<ul style="list-style-type: none"> The application of the DeeperCut [66] feature detector architecture, that was originally designed for human pose estimation, to animal pose estimation.
LEAP [128]	2019	✗	Mice, Flies	2D	✗	<ul style="list-style-type: none"> The design of a CNN architecture inspired by three human pose estimation architectures [118, 154, 170]. The CNN is shallow and is trained from scratch to improve inference speed compared to DeepLabCut at the expense of less robustness and requiring more training data to achieve the same performance.
DeepPoseKit [54]	2019	✓(if not occluded)	Flies, Locusts, Zebras	2D	✗	<ul style="list-style-type: none"> The development of a stacked DenseNet architecture [118] [71] [64] to improve speed and robustness.
DeepFly3D [56]	2019	✗	Flies, Humans	3D	✓	<ul style="list-style-type: none"> The adaptation of a stacked hourglass architecture [118] to permit 3D pose estimation using multiple cameras.
Anipose [81]	2021	✗	Flies, Mice, Humans	3D	✓	<ul style="list-style-type: none"> The introduction of filters to improve 2D tracking and a novel triangulation procedure for 3D pose estimation using multiple cameras.
LiftPose3D [52]	2021	✗	Flies, Mice, Monkeys	3D	✗	<ul style="list-style-type: none"> The adaptation of an architecture designed for lifting 2D human pose into 3D [107] for monocular 3D animal pose estimation.
Multi-animal DeepLabCut [90]	2022	✓	Mice, Monkeys, Fish	2D/3D	✓	<ul style="list-style-type: none"> The development of a multi-task architecture which identifies keypoints, assembles them to predict limbs, then assigns them to individuals. This formulation allows for the tracking of multiple animals in one scene.
SLEAP [129]	2022	✓	Mice, Flies, Bees, Gerbils	2D	✗	<ul style="list-style-type: none"> The design of a novel multi-animal pose tracking system that incorporates multiple CNN architectures and approaches for part grouping and identity tracking.

Table 8. Animal Pose Estimation Methods. Pink: supervised.

– Self-supervised Feature Extraction (Selfee) [73] (Figure 11), trains a network to extract suitable classification features from unlabeled videos (about 5 million). Two Siamese CNNs based on ResNet-50 learn a discriminative feature representation of behavior with a training rate that is faster (8 hours on one GPU) than modern self-supervised models. Note that this paper also included a classification example that used labels.

6 DISCUSSION AND FUTURE DIRECTIONS

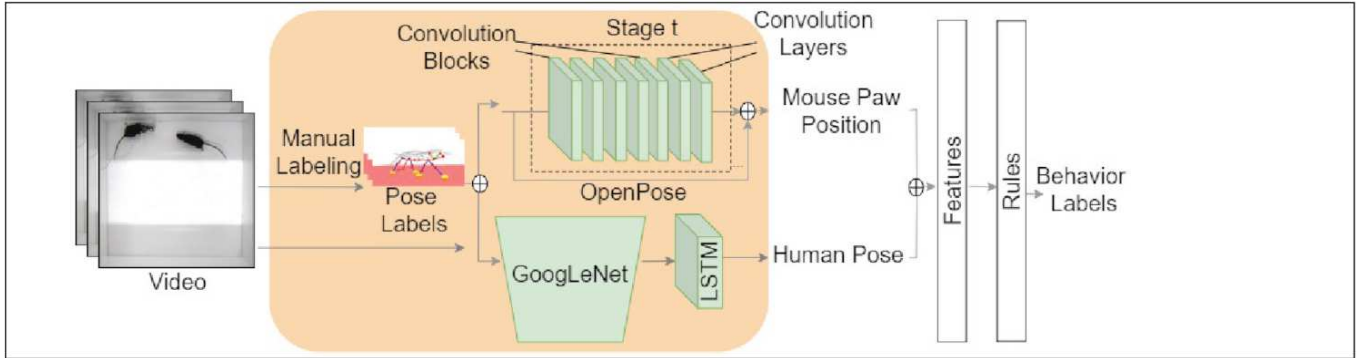
This section discusses future research that investigates adaptations of action recognition for animal behavior classification.

Action recognition has many practical applications as many professions use automated methods to interpret motion from publicly available or privately acquired videos. Although we are motivated by problems with behavior analysis in neuroscience, these research topics are relevant to several application spaces. Recognizing player movements in gaming [13], monitoring infants [114], preventative healthcare for the elderly, and hand-object pose estimation in augmented and virtual reality environments [39] are examples.

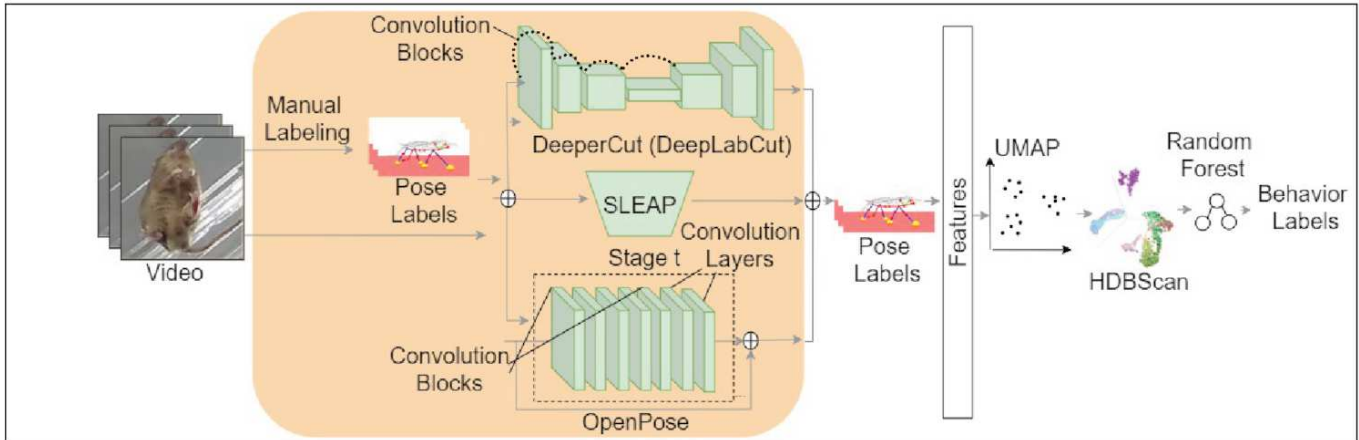
There are opportunities to further evaluate human action recognition methods on animal behavior classification problems. Human action recognition methods are mature compared to emerging developments in animal behavior classification [74]. Adapting CNN-based action recognition methods not yet considered in this domain

Method	Year	Pose Based	Social	Validated	Depth Cam.	Key Contribution(s)
JAABA [79]	2013	✓	✓	Mice, Flies	✗	<ul style="list-style-type: none"> The development of a supervised behavior classification system usable by biologists. A set of per-frame features are computed from the pose trajectories that are input to an optimized GentleBoost learning algorithm [43].
MotionMapper [11]	2014	✗	✓	Flies	✗	<ul style="list-style-type: none"> The design of an unsupervised behavior classification pipeline in invertebrates in which frames are segmented, scaled, aligned, then decomposed via PCA. A spectrogram is created for each postural mode, then each point in time is mapped to a 2D plane using t-SNE. Peaks are identified after the application of a watershed transform.
MoSeq [171, 172]	2015	✗	✗	Mice	✓	<ul style="list-style-type: none"> The design of an unsupervised approach to identify behavioral modules in vertebrates. After compressing mice videos using PCA, an AR-HMM is used to segment the representation into discrete behavioral syllables.
DeepBehavior [4]	2019	✓	✓	Mice, Humans	✗	<ul style="list-style-type: none"> The adaptation of GoogLeNet [148] and YOLO-v3 [134] CNN architectures to identify rodent behaviors individually and socially, respectively.
BehaveNet [8]	2019	✗	✗	Mice	✗	<ul style="list-style-type: none"> The introduction of a probabilistic framework for the unsupervised analysis of behavioral videos and neural activity. The use of a CAE to compress videos before they are segmented into discrete behavioral syllables using an AR-HMM. A generative model that can be used to simulate behavioral videos given neural activity.
B-SoiD [61]	2021	✓	✗	Mice	✗	<ul style="list-style-type: none"> The dimensionality reduction of pose features produced by DeepLabCut [108] using UMAP. The use of HDBScan to cluster the embedded features and the subsequent training of a random forest classifier to predict behaviors directly from high-dimensional pose features.
SimBA [121]	2020	✓	✓	Mice, Rats	✗	<ul style="list-style-type: none"> The design of a pose-based approach to rodent social behavior analysis with tools to increase ease-of-use for behavioral neuroscientists. The classification of behaviors based on positions of recognized joints.
MARS [139]	2021	✓	✓	Mice	✗	<ul style="list-style-type: none"> The development of a pose-based approach to recognize social behaviors between a black and white mouse.
DeepEthogram [14]	2021	✗	✓	Mice, Flies	✗	<ul style="list-style-type: none"> The design of a novel supervised approach that operates on raw pixel values. Optical flow is estimated from video clips using MotionNet [180], flow and spatial features are compressed, and then a sequence model estimates the probability of each behavior in each frame.

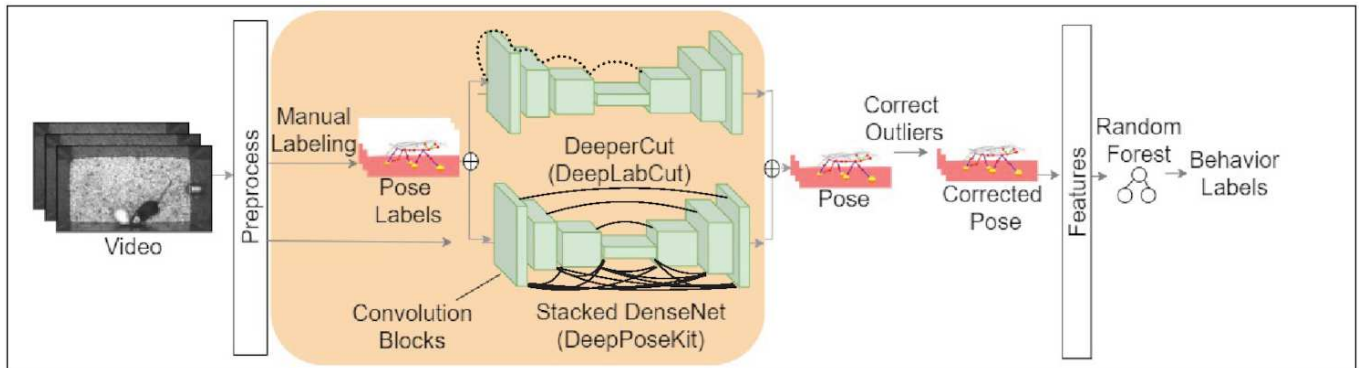
Table 9. Animal Behavior Classification Frameworks. Pink: supervised, Blue: unsupervised



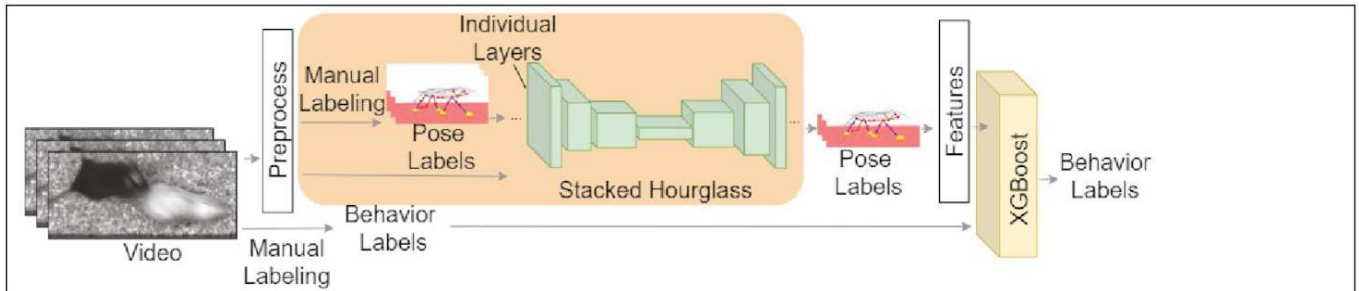
DeepBehavior [4]



Behavioral Segmentation of Open Field in DeepLabCut (B-SOiD) [61]



Simple Behavior Analysis (SimBA) [121]



Mouse Action Recognition System (MARS) [139]

Fig. 9. Pose-based Animal Behavior Classification Frameworks

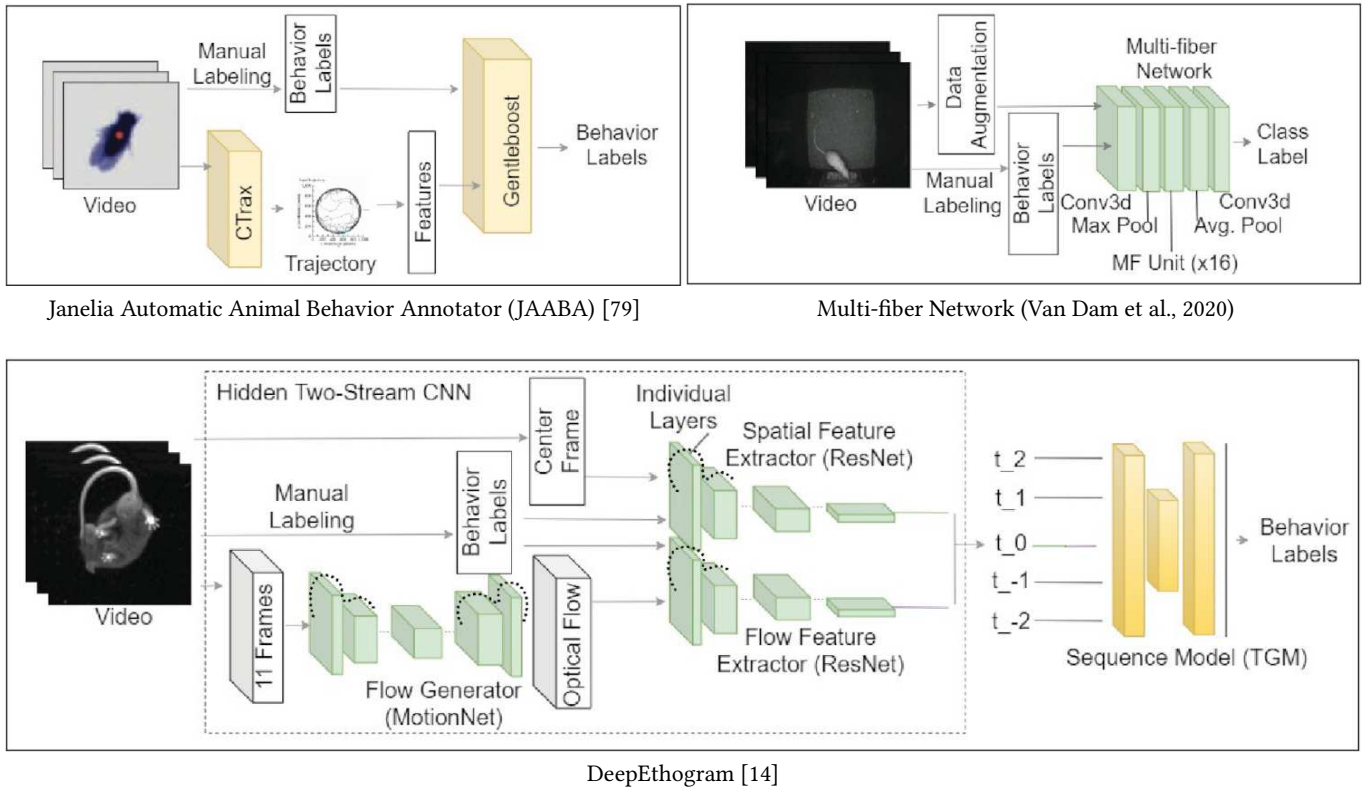


Fig. 10. Supervised Animal Behavior Classification Frameworks that Operate on Pixel Values without Pose Estimation

would be beneficial to address domain specific problems like occlusion from hidden limbs on small subjects, as well as historical challenges like processing high-resolution videos. Action recognition methods work on trimmed videos while many animal behavior methods operate on untrimmed videos with labeled frames. Frames with a broad range of non-class activities may be indicated by a single background class. Accurate evaluation of new methods on existing benchmark datasets will require special handling when the data varies between these domains. Many CNN architectures operate on low resolution videos. Higher resolution data, or increased kernel sizes (for detecting long range dependencies) increase computation time. There is a need to consider CNN-based systems that are customized to address the speed accuracy trade-off. The following research topics are relevant:

Fully Unsupervised Behavior Classification: Behavior analysis is important for diagnosing and treating neurological disorders [109]. The human action recognition techniques we reviewed were supervised or semi-supervised, requiring labeled videos. Manual labeling of videos is time consuming and inconsistent [55]. Unsupervised animal behavior classification systems [8, 11, 73, 171, 172] are few, and open challenges remain. Our taxonomy (Section 5.4) shows that many methods that are broadly classified as unsupervised are discriminative and pose-based. Many steps still require hand-crafted features, or labels in complex systems. Unsupervised classification

systems would remove manual scoring and inconsistencies that might skew results [14, 55, 139]. In addition, new micro-scale behaviors that are not pre-defined in a behavior collection may be discovered. Approaches that operate on unstructured data should be able to identify behaviors at different time scales and organize behavior in a hierarchical structure.

Action Recognition in Crowds and Complex Social Environments: Many behavioral studies aim to understand complex social behaviors of multiple subjects in intricate environments. In these scenarios, identifying the behavior of multiple subjects performing individual actions in the same frame is challenging. Pose-based action recognition systems that use two-stage inference are more prone to errors when there are multiple overlapping body parts. A common error is the assignment of the same limbs to multiple subjects. In the domain of animal behavior classification, CS-IGANet and other works [20] can classify multi-subject behaviors in social datasets like the CRIM13 resident-intruder mouse [20] dataset. However, these approaches do not predict individual actions of each subject. SIPEC [105] is one of the first examples to have success identifying behaviors of individual subjects in a social setting. There is a need to investigate networks that evaluate dense activity (swarms) in *in-the-wild* conditions.

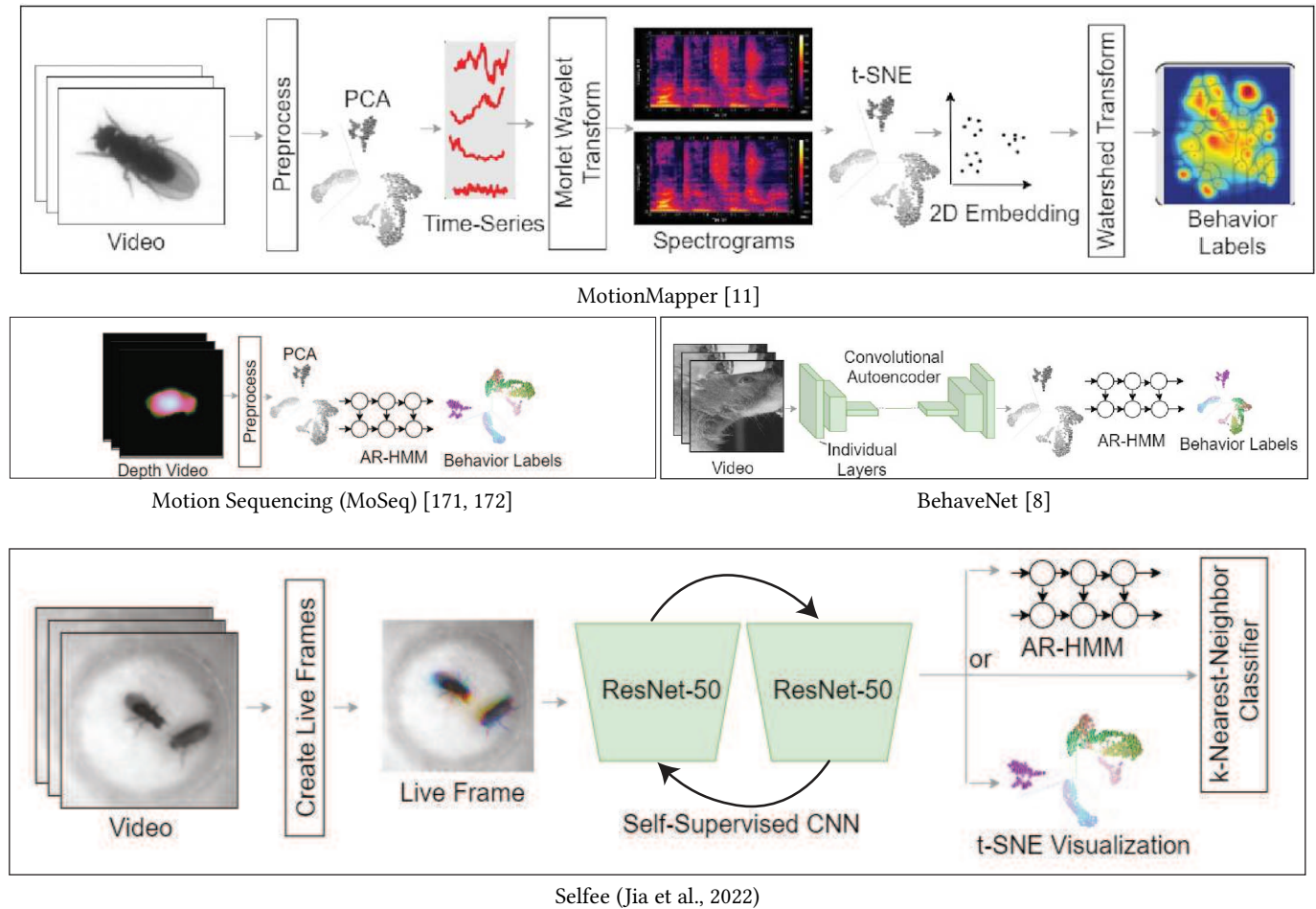


Fig. 11. Unsupervised Animal Behavior Classification Frameworks that Operate on Pixel Values without Pose Estimation.

Robust Multi-modal Action Recognition: Multimodal data capture has been used to describe an animal’s dynamics in social interactions. Multi-modal sensing for behavior recognition is important as a more complete behavior representation may be achieved by combining heterogeneous information from different sensory devices. However, it is a challenge to fuse and work with motion information across different sensory devices, and when there are significant variations in environmental lighting conditions. Networks that operate on multimodal data from different imaging modalities would be effective for interoperability.

7 CONCLUSION

Automated classification of activity performed by humans in videos is an important problem in computer vision with applications in many fields. We presented a thorough and detailed review of CNN architectures developed for two related tasks: human action recognition, and human pose estimation. We traced the development of these network architectures, examining design decisions that increased performance on benchmark image and video datasets. We

focused our paper on techniques that have been modified for animal behavior classification tasks. Our taxonomy for animal behavior classification frameworks is more comprehensive than others because we consider model inputs and system components that influence more varied levels of supervision. We discussed and compared the components of several of these behavior classification systems, highlighting challenges and future research directions. We believe this survey will inspire future work in action recognition, its adaptation for animal behavior classification, and new evaluation metrics that compare neural network performance across different levels of supervision.

REFERENCES

- [1] Yasemin Altun, Ioannis Tsochantaridis, and Thomas Hofmann. 2003. Hidden Markov Support Vector Machines. In *Proceedings of the Twentieth International Conference on International Conference on Machine Learning (ICML’03)*. AAAI Press, Washington, DC, USA, 3â€–10.
- [2] David J Anderson and Pietro Perona. 2014. Toward a science of computational ethology. *Neuron* 84, 1 (2014), 18–31.
- [3] M. Andriluka, L. Pishchulin, P. Gehler, and B. Schiele. 2014. 2D Human Pose Estimation: New Benchmark and State of the Art Analysis. In *2014 IEEE Conference on Computer Vision and Pattern Recognition (CVPR)*. IEEE Computer Society, Los

- Alamitos, CA, USA, 3686–3693. <https://doi.org/10.1109/CVPR.2014.471>
- [4] Ahmet Arac, Pingping Zhao, Bruce H. Dobkin, S. Thomas Carmichael, and Peyman Golshani. 2019. DeepBehavior: A Deep Learning Toolbox for Automated Analysis of Animal and Human Behavior Imaging Data. *Frontiers in Systems Neuroscience* 13 (2019), 20. <https://doi.org/10.3389/fnysys.2019.00020>
- [5] Mohamad Babiker, Othman O. Khalifa, Kyaw Kyaw Htike, Aisha Hassan, and Muhamed Zaharadeen. 2017. Automated daily human activity recognition for video surveillance using neural network. In *2017 IEEE 4th International Conference on Smart Instrumentation, Measurement and Application (ICSIMA)*. 1–5. <https://doi.org/10.1109/ICSIMA.2017.8312024>
- [6] Vijay Badrinarayanan, Alex Kendall, and Roberto Cipolla. 2017. SegNet: A Deep Convolutional Encoder-Decoder Architecture for Image Segmentation. *IEEE Transactions on Pattern Analysis and Machine Intelligence* 39, 12 (2017), 2481–2495. <https://doi.org/10.1109/TPAMI.2016.2644615>
- [7] Simon Baker and Iain Matthews. 2004. Lucas-Kanade 20 Years On: A Unifying Framework. *International Journal of Computer Vision* 56, 3 (01 Feb 2004), 221–255. <https://doi.org/10.1023/B:VISI.0000011205.11775.fd>
- [8] Eleanor Batty, Matthew Whiteway, Shreya Saxena, Dan Biderman, Taiga Abe, Simon Musall, Winthrop Gillis, Jeffrey Markowitz, Anne Churchland, John P. Cunningham, Sandeep R Datta, Scott Linderman, and Liam Paninski. 2019. BehaveNet: nonlinear embedding and Bayesian neural decoding of behavioral videos. In *Advances in Neural Information Processing Systems*, H. Wallach, H. Larochelle, A. Beygelzimer, F. d'Alché-Buc, E. Fox, and R. Garnett (Eds.), Vol. 32. Curran Associates, Inc., Red Hook, NY, USA.
- [9] Vasileios Belagiannis and Andrew Zisserman. 2017. Recurrent Human Pose Estimation. In *2017 12th IEEE International Conference on Automatic Face and Gesture Recognition (FG 2017)* (Washington, DC, DC, USA). IEEE Press, New York, NY, USA, 468â–475. <https://doi.org/10.1109/FG.2017.64>
- [10] Gordon Berman. 2018. Measuring behavior across scales. *BMC Biology* 16 (02 2018). <https://doi.org/10.1186/s12915-018-0494-7>
- [11] Gordon Berman, Daniel Choi, William Bialek, and Joshua Shaevitz. 2014. Mapping the stereotyped behaviour of free moving fruit flies. *Journal of The Royal Society Interface* 11 (08 2014), 20140672. <https://doi.org/10.1098/rsif.2014.0672>
- [12] Christopher M. Bishop. 2006. *Pattern Recognition and Machine Learning (Information Science and Statistics)*. Springer-Verlag, Berlin, Heidelberg.
- [13] V. Bloom, D. Makris, and V. Argyriou. 2012. G3D: A gaming action dataset and real time action recognition evaluation framework. In *2012 IEEE Computer Society Conference on Computer Vision and Pattern Recognition Workshops (CVPR Workshops)*. IEEE Computer Society, Los Alamitos, CA, USA, 7–12. <https://doi.org/10.1109/CVPRW.2012.6239175>
- [14] James P Bohmslav, Nivanthika K Wimalasena, Kelsey J Clausing, Yu Y Dai, David A Yarmolinsky, Tomás Cruz, M Eugenia Kashlan, Adam Dand Chiappe, Lauren L Orefice, Clifford J Woolf, et al. 2021. DeepEthogram, a machine learning pipeline for supervised behavior classification from raw pixels. *Elife* 10 (2021), e63377.
- [15] Kristin Branson, Alice Robie, John A. Bender, Pietro Perona, and Michael H. Dickinson. 2009. High-throughput Ethomics in Large Groups of *Drosophila*. *Nature methods* 6 (2009), 451–457.
- [16] Biagio Brattoli, Uta Büchler, Michael Dorkenwald, Philipp Reiser, Linard Filli, Fritjof Helmchen, Anna-Sophia Wahl, and Björn Ommer. 2021. Unsupervised behaviour analysis and magnification (uBAM) using deep learning. *Nature Machine Intelligence* 3, 6 (2021), 495–506.
- [17] André E. X. Brown, Eviatar I. Yemini, Laura J. Grundy, Tadas Jucikas, and William R. Schafer. 2013. A dictionary of behavioral motifs reveals clusters of genes affecting *Caenorhabditis elegans* locomotion. *Proceedings of the National Academy of Sciences* 110, 2 (2013), 791–796. <https://doi.org/10.1073/pnas.1211447110> arXiv:<https://www.pnas.org/doi/pdf/10.1073/pnas.1211447110>
- [18] Thomas Brox, Andrés Bruhn, Nils Papenberger, and Joachim Weickert. 2004. High Accuracy Optical Flow Estimation Based on a Theory for Warping. In *Computer Vision - ECCV 2004*, Tomás Pajdla and Jiří Matas (Eds.), Springer Berlin Heidelberg, Berlin, Heidelberg, 25–36.
- [19] Tekin Bugra, Katircioglu Isinsu, Salzmann Mathieu, Lepetit Vincent, and Fua Pascal. 2016. Structured Prediction of 3D Human Pose with Deep Neural Networks. In *Proceedings of the British Machine Vision Conference (BMVC)*, Edwin R. Hancock Richard C. Wilson and William A. P. Smith (Eds.). BMVA Press, York, UK, Article 130, 11 pages. <https://doi.org/10.5244/C.30.130>
- [20] Xavier P. Burgos-Artizzu, Piotr Dollár, Dayu Lin, David J. Anderson, and Pietro Perona. 2012. Social Behavior Recognition in Continuous Video. In *Proceedings of the 2012 IEEE Conference on Computer Vision and Pattern Recognition (CVPR)* (CVPR '12). IEEE Computer Society, USA, 1322â–1329.
- [21] Ricardo J. G. B. Campello, Davoud Moulavi, Arthur Zimek, and Jörg Sander. 2015. Hierarchical Density Estimates for Data Clustering, Visualization, and Outlier Detection. *ACM Trans. Knowl. Discov. Data* 10, 1, Article 5 (jul 2015), 51 pages. <https://doi.org/10.1145/2733381>
- [22] Z. Cao, G. Hidalgo, T. Simon, S. Wei, and Y. Sheikh. 2021. OpenPose: Real-time Multi-Person 2D Pose Estimation Using Part Affinity Fields. *IEEE Transactions on Pattern Analysis & Machine Intelligence* 43, 01 (jan 2021), 172–186. <https://doi.org/10.1109/TPAMI.2019.2929257>
- [23] Joao Carreira, Eric Noland, Andras Banki-Horvath, Chloe Hillier, and Andrew Zisserman. 2018. A Short Note about Kinetics-600. <https://doi.org/10.48550/ARXIV.1808.01340>
- [24] J. Carreira and A. Zisserman. 2017. Quo Vadis, Action Recognition? A New Model and the Kinetics Dataset. In *2017 IEEE Conference on Computer Vision and Pattern Recognition (CVPR)*. IEEE Computer Society, Los Alamitos, CA, USA, 4724–4733. <https://doi.org/10.1109/CVPR.2017.502>
- [25] Tianqi Chen and Carlos Guestrin. 2016. XGBoost: A Scalable Tree Boosting System. In *Proceedings of the 22nd ACM SIGKDD International Conference on Knowledge Discovery and Data Mining* (San Francisco, California, USA) (KDD '16). Association for Computing Machinery, New York, NY, USA, 785â–794. <https://doi.org/10.1145/2939672.2939785>
- [26] Xianjie Chen and Alan Yuille. 2014. Articulated Pose Estimation by a Graphical Model with Image Dependent Pairwise Relations. In *Proceedings of the 27th International Conference on Neural Information Processing Systems - Volume 1* (Montreal, Canada) (NIPS'14). MIT Press, Cambridge, MA, USA, 1736â–1744.
- [27] Yunpeng Chen, Yannis Kalantidis, Jianshu Li, Shuicheng Yan, and Jiashi Feng. 2018. Multi-fiber Networks for Video Recognition. In *Computer Vision - ECCV 2018*, Vittorio Ferrari, Martial Hebert, Cristian Sminchisescu, and Yair Weiss (Eds.). Springer International Publishing, Cham, 364–380.
- [28] Yucheng Chen, Yingli Tian, and Mingyi He. 2020. Monocular human pose estimation: A survey of deep learning-based methods. *Computer Vision and Image Understanding* 192 (2020), 102897. <https://doi.org/10.1016/j.cviu.2019.102897>
- [29] Zexin Chen, Ruihan Zhang, Ruihan Zhang, Yu Eva Zhang, Haowen Zhou, Hao-Shu Fang, Rachel Rock, Aneesh Bal, Nancy Padilla-Coreano, Laurel Keyes, Kay Tye, and Cewu Lu. 2020. AlphaTracker: A Multi-Animal Tracking and Behavioral Analysis Tool. <https://doi.org/10.1101/2020.12.04.405159>
- [30] F. Chollet. 2017. Xception: Deep learning with depthwise separable convolutions. In *2017 IEEE Conference on Computer Vision and Pattern Recognition (CVPR)*. IEEE Computer Society, Los Alamitos, CA, USA, 1800–1807. <https://doi.org/10.1109/CVPR.2017.195>
- [31] Junyoung Chung, Caglar Gulcehre, Kyunghyun Cho, and Yoshua Bengio. 2014. Empirical evaluation of gated recurrent neural networks on sequence modeling. Genaro A Coria-Avila, James G Pfau, Agustín Orihuela, Adriana Domínguez-Oliva, Nancy José-Pérez, Laura Astrid Hernández, and Daniel Mota-Rojas. 2022. The Neurobiology of Behavior and Its Applicability for Animal Welfare: A Review. *Animals* 12, 7 (2022), 928.
- [32] Heiko Dankert, Liming Wang, Eric Hoopfer, David Anderson, and Pietro Perona. 2009. Automated Monitoring and Analysis of Social Behavior in *Drosophila*. *Nature methods* 6 (05 2009), 297–303. <https://doi.org/10.1038/nmeth.1310>
- [33] Sandeep Robert Datta, David J. Anderson, Kristin Branson, Pietro Perona, and Andrew Leifer. 2019. Computational Neuroethology: A Call to Action. *Neuron* 104, 1 (2019), 11–24. <https://doi.org/10.1016/j.neuron.2019.09.038>
- [34] Fabrice de Chaumont, Elodie Ey, Nicolas Torquet, Thibault Lagache, Stéphane Dallongeville, Albane Imbert, Thierry Legou, Anne-Marie Le Sourd, Philippe Faure, Thomas Bourgeron, and Jean-Christophe Olivo-Marin. 2019. Real-time analysis of the behaviour of groups of mice via a depth-sensing camera and machine learning. *Nature Biomedical Engineering* 3, 11 (01 Nov 2019), 930–942. <https://doi.org/10.1038/s41551-019-0396-1>
- [35] Jia Deng, Wei Dong, Richard Socher, Li-Jia Li, Kai Li, and Li Fei-Fei. 2009. ImageNet: A large-scale hierarchical image database. In *2009 IEEE Computer Society Conference on Computer Vision and Pattern Recognition Workshops (CVPR Workshops)*. IEEE Computer Society, Los Alamitos, CA, USA, 248–255. <https://doi.org/10.1109/CVPR.2009.5206848>
- [36] Ali Diba, Ali Pazandeh, and Luc Van Gool. 2016. Efficient Two-Stream Motion and Appearance 3D CNNs for Video Classification.
- [37] Jeff Donahue, Yangqing Jia, Oriol Vinyals, Judy Hoffman, Ning Zhang, Eric Tzeng, and Trevor Darrell. 2014. DeCAF: A Deep Convolutional Activation Feature for Generic Visual Recognition. In *Proceedings of the 31st International Conference on Machine Learning - Volume 32 (ICML'14)*. JMLR.org, Beijing, China, 1â–6.
- [38] Bardia Doosti, Shujon Naha, Majid Mirbagheri, and David J Crandall. 2020. HOPE-Net: A Graph-Based Model for Hand-Object Pose Estimation. In *2020 IEEE/CVF Conference on Computer Vision and Pattern Recognition (CVPR)*. IEEE Computer Society, Los Alamitos, CA, USA, 6607–6616. <https://doi.org/10.1109/CVPR42600.2020.00664>
- [39] Mark Everingham, Luc Van Gool, Christopher K. I. Williams, John M. Winn, and Andrew Zisserman. 2009. The Pascal Visual Object Classes (VOC) Challenge. *International Journal of Computer Vision* 88 (2009), 303–338.

- [41] C. Feichtenhofer, A. Pinz, and A. Zisserman. 2016. Convolutional Two-Stream Network Fusion for Video Action Recognition. In *2016 IEEE Conference on Computer Vision and Pattern Recognition (CVPR)*. IEEE Computer Society, Los Alamitos, CA, USA, 1933–1941. <https://doi.org/10.1109/CVPR.2016.213>
- [42] Brendan J. Frey and Delbert Dueck. 2007. Clustering by Passing Messages Between Data Points. *Science* 315, 5814 (2007), 972–976. <https://doi.org/10.1126/science.1136800> arXiv:<https://www.science.org/doi/pdf/10.1126/science.1136800>
- [43] Jerome Friedman, Trevor Hastie, and Robert Tibshirani. 2000. Additive Logistic Regression: A Statistical View of Boosting. *The Annals of Statistics* 28 (04 2000), 337–407. <https://doi.org/10.1214/aos/1016218223>
- [44] Keinosuke Fukunaga. 2013. *Introduction to statistical pattern recognition*. Elsevier, USA.
- [45] Christopher J Gabriel, Zachary Zeidler, Benita Jin, Changliang Guo, Caitlin M Goodpaster, Adrienne Q Kashay, Anna Wu, Molly Delaney, Jovian Cheung, Lauren E DiFazio, Melissa J Sharpe, Daniel Aharoni, Scott A Wilke, and Laura A DeNardo. 2022. BehaviorDEPOT is a simple, flexible tool for automated behavioral detection based on markerless pose tracking. *eLife* 11 (aug 2022), e74314. <https://doi.org/10.7554/eLife.74314>
- [46] E. Garrote, T. Serre, H. Jhuang, H. Kuehne, and T. Poggio. 2011. HMDB: A large video database for human motion recognition. In *2011 IEEE International Conference on Computer Vision (ICCV 2011)*. IEEE Computer Society, Los Alamitos, CA, USA, 2556–2563. <https://doi.org/10.1109/ICCV.2011.6126543>
- [47] Luca Giancardo, Diego Sona, Huiping Huang, Sara Sannino, Francesca Managò, Diego Scheggia, Francesco Papaleo, and Vittorio Murino. 2013. Automatic visual tracking and social behaviour analysis with multiple mice. *PLoS one* 8, 9 (2013), e74557.
- [48] R. Girshick. 2015. Fast R-CNN. In *2015 IEEE International Conference on Computer Vision (ICCV)*. IEEE Computer Society, Los Alamitos, CA, USA, 1440–1448. <https://doi.org/10.1109/ICCV.2015.169>
- [49] R. Girshick, J. Donahue, T. Darrell, and J. Malik. 2014. Rich Feature Hierarchies for Accurate Object Detection and Semantic Segmentation. In *2014 IEEE Conference on Computer Vision and Pattern Recognition (CVPR)*. IEEE Computer Society, Los Alamitos, CA, USA, 580–587. <https://doi.org/10.1109/CVPR.2014.81>
- [50] M A Goodale and A D Milner. 1992. Separate visual pathways for perception and action. *Trends Neurosci* 15, 1 (jan 1992), 20–25.
- [51] Ian J. Goodfellow, Yoshua Bengio, and Aaron Courville. 2016. *Deep Learning*. MIT Press, Cambridge, MA, USA. <http://www.deeplearningbook.org>.
- [52] Adam Gosztołai, Semih Günel, Victor Lobato Ríos, Marco Pietro Abrate, Daniel Morales, Helge Rhodin, Pascal Fua, and Pavan Ramdya. 2021. LiftPose3D, a deep learning-based approach for transforming 2D to 3D pose in laboratory animals. *Nature methods* 18, 8 (2021), 975.
- [53] Pierre Goupillaud, Alex Grossmann, and Jean Morlet. 1984. Cycle-octave and related transforms in seismic signal analysis. *Geoexploration* 23, 1 (1984), 85–102.
- [54] Jacob M Graving, Daniel Chae, Hemal Naik, Liang Li, Benjamin Koger, Blair R Costelloe, and Iain D Couzin. 2019. DeepPoseKit, a software toolkit for fast and robust animal pose estimation using deep learning. *eLife* 8 (oct 2019), e47994. <https://doi.org/10.7554/eLife.47994>
- [55] Maria Gulinello, Heather A Mitchell, Qiang Chang, W Timothy O'Brien, Zhaolan Zhou, Ted Abel, Li Wang, Joshua G Corbin, Surabi Veeraragavan, Rodney C Samaco, et al. 2019. Rigor and reproducibility in rodent behavioral research. *Neurobiology of learning and memory* 165 (2019), 106780.
- [56] Semih Gâijnel, Helge Rhodin, Daniel Morales, João Campagnolo, Pavan Ramdya, and Pascal Fua. 2019. DeepFly3D, a deep learning-based approach for 3D limb and appendage tracking in tethered, adult *Drosophila*. *eLife* 8 (oct 2019), e48571. <https://doi.org/10.7554/eLife.48571>
- [57] Yaning Han, Kang Huang, Ke Chen, Hongli Pan, Furong Ju, Yueyue Long, Gao Gao, Runlong Wu, Aimin Wang, Liping Wang, et al. 2022. MouseVenue3D: A Markerless Three-Dimension Behavioral Tracking System for Matching Two-Photon Brain Imaging in Free-Moving Mice. *Neuroscience Bulletin* 38, 3 (2022), 303–317. <https://doi.org/10.1016/j.cviu.2022.103483>
- [58] K. He, X. Zhang, S. Ren, and J. Sun. 2016. Deep Residual Learning for Image Recognition. In *2016 IEEE Conference on Computer Vision and Pattern Recognition (CVPR)*. IEEE Computer Society, Los Alamitos, CA, USA, 770–778. <https://doi.org/10.1109/CVPR.2016.90>
- [59] F. Heilbron, V. Escorcia, B. Ghanem, and J. Niebles. 2015. ActivityNet: A large-scale video benchmark for human activity understanding. In *2015 IEEE Conference on Computer Vision and Pattern Recognition (CVPR)*. IEEE Computer Society, Los Alamitos, CA, USA, 961–970. <https://doi.org/10.1109/CVPR.2015.7298698>
- [60] Weizhe Hong, Ann Kennedy, Xavier P Burgos-Artizzu, Moriel Zelikowsky, Santiago G Navonne, Pietro Perona, and David J Anderson. 2015. Automated measurement of mouse social behaviors using depth sensing, video tracking, and machine learning. *Proceedings of the National Academy of Sciences* 112, 38 (2015), E5351–E5360.
- [61] Alexander I Hsu and Eric A Yttri. 2021. B-SOId, an open-source unsupervised algorithm for identification and fast prediction of behaviors. *Nature communications* 12, 1 (2021), 1–13.
- [62] Jie Hu, Li Shen, and Gang Sun. 2018. Squeeze-and-Excitation Networks. In *2018 IEEE/CVF Conference on Computer Vision and Pattern Recognition (CVPR)*. IEEE Computer Society, Los Alamitos, CA, USA, 7132–7141. <https://doi.org/10.1109/CVPR.2018.00745>
- [63] Yujia Hu, Carrie R. Ferrario, Alexander D. Maitland, Rita B. Ionides, Anjesh Ghimire, Brendon Watson, Kenichi Iwasaki, Hope White, Yitao Xi, Jie Zhou, and Bing Ye. 2022. LabGym: quantification of user-defined animal behaviors using learning-based holistic assessment. <https://doi.org/10.1101/2022.02.17.480911>
- [64] G. Huang, Z. Liu, L. Van Der Maaten, and K. Q. Weinberger. 2017. Densely Connected Convolutional Networks. In *2017 IEEE Conference on Computer Vision and Pattern Recognition (CVPR)*. IEEE Computer Society, Los Alamitos, CA, USA, 2261–2269. <https://doi.org/10.1109/CVPR.2017.243>
- [65] J. Huang, V. Rathod, C. Sun, M. Zhu, A. Korattikara, A. Fathi, I. Fischer, Z. Wojna, Y. Song, S. Guadarrama, and K. Murphy. 2017. Speed/Accuracy Trade-Offs for Modern Convolutional Object Detectors. In *2017 IEEE Conference on Computer Vision and Pattern Recognition (CVPR)*. IEEE Computer Society, Los Alamitos, CA, USA, 3296–3297. <https://doi.org/10.1109/CVPR.2017.351>
- [66] Eldar Insafutdinov, Leonid Pishchulin, Bjoern Andres, Mykhaylo Andriluka, and Bernt Schiele. 2016. DeeperCut: A Deeper, Stronger, and Faster Multi-person Pose Estimation Model. In *Computer Vision – ECCV 2016*, Bastian Leibe, Jiri Matas, Nicu Sebe, and Max Welling (Eds.). Springer International Publishing, Cham, 34–50.
- [67] Catalin Ionescu, Dragos Papava, Vlad Olaru, and Cristian Sminchisescu. 2014. Human3.6M: Large Scale Datasets and Predictive Methods for 3D Human Sensing in Natural Environments. *IEEE Transactions on Pattern Analysis and Machine Intelligence* 36, 7 (2014), 1325–1339. <https://doi.org/10.1109/TPAMI.2013.248>
- [68] Max Jaderberg, Karen Simonyan, Andrew Zisserman, and Koray Kavukcuoglu. 2015. Spatial Transformer Networks. In *Proceedings of the 28th International Conference on Neural Information Processing Systems - Volume 2 (Montreal, Canada) (NIPS'15)*. MIT Press, Cambridge, MA, USA, 2017–2025.
- [69] Arjun Jain, Jonathan Tompson, Mykhaylo Andriluka, Graham W. Taylor, and Christoph Bregler. 2014. Learning Human Pose Estimation Features with Convolutional Networks. In *2nd International Conference on Learning Representations, ICLR 2014, Banff, AB, Canada, April 14-16, 2014, Conference Track Proceedings*, Yoshua Bengio and Yann LeCun (Eds.). OpenReview.net, Banff, AB, Canada, 11. <http://arxiv.org/abs/1312.7302>
- [70] Arjun Jain, Jonathan Tompson, Yann LeCun, and Christoph Bregler. 2015. MoD-ep: A Deep Learning Framework Using Motion Features for Human Pose Estimation. In *Computer Vision – ACCV 2014*, Daniel Cremers, Ian Reid, Hideo Saito, and Ming-Hsuan Yang (Eds.). Springer International Publishing, Cham, 302–315.
- [71] S. Jegou, M. Drozdal, D. Vazquez, A. Romero, and Y. Bengio. 2017. The One Hundred Layers Tiramisu: Fully Convolutional DenseNets for Semantic Segmentation. In *2017 IEEE Conference on Computer Vision and Pattern Recognition Workshops (CVPRW)*. IEEE Computer Society, Los Alamitos, CA, USA, 1175–1183. <https://doi.org/10.1109/CVPRW.2017.156>
- [72] Hueihan Jhuang, Estibaliz Garrote, Xinlin Yu, Vinita Khilnani, Tomaso Poggio, Andrew D Steele, and Thomas Serre. 2010. Automated home-cage behavioural phenotyping of mice. *Nature communications* 1, 1 (2010), 1–10.
- [73] Yinjun Jia, Shuaishuai Li, Xuan Guo, Bo Lei, Junjing Hu, Xiao-Hong Xu, and Wei Zhang. 2022. Selfee, self-supervised features extraction of animal behaviors. *Elife* 11 (2022), e76218.
- [74] Le Jiang, Caleb Lee, Divyang Teotia, and Sarah Ostadabbas. 2022. Animal pose estimation: A closer look at the state-of-the-art, existing gaps and opportunities. *Computer Vision and Image Understanding* 222 (2022), 103483. <https://doi.org/10.1016/j.cviu.2022.103483>
- [75] Y.-G. Jiang, J. Liu, A. Roshan Zamir, G. Toderici, I. Laptev, M. Shah, and R. Sukthankar. 2014. THUMOS Challenge: Action Recognition with a Large Number of Classes. <http://csrcv.ucf.edu/THUMOS14/>. (2014).
- [76] Yu-Gang Jiang, Guangnan Ye, Shih-Fu Chang, Daniel Ellis, and Alexander C. Loui. 2011. Consumer Video Understanding: A Benchmark Database and an Evaluation of Human and Machine Performance. In *Proceedings of the 1st ACM International Conference on Multimedia Retrieval (Trento, Italy) (ICMR '11)*. Association for Computing Machinery, New York, NY, USA, Article 29, 8 pages. <https://doi.org/10.1145/1991996.1992025>
- [77] Sam Johnson and Mark Everingham. 2010. Clustered Pose and Non-linear Appearance Models for Human Pose Estimation. In *Proceedings of the British Machine Vision Conference*. BMVA Press, Aberystwyth, UK, 12.1–12.11. doi:10.5244/C.24.12.
- [78] S. Johnson and M. Everingham. 2011. Learning Effective Human Pose Estimation from Inaccurate Annotation. In *Proceedings of the 2011 IEEE Conference on Computer Vision and Pattern Recognition (CVPR '11)*. IEEE Computer Society, USA, 1465–1472. <https://doi.org/10.1109/CVPR.2011.5995318>

- [79] Mayank Kabra, Alice A Robie, Marta Rivera-Alba, Steven Branson, and Kristin Branson. 2013. JAABA: interactive machine learning for automatic annotation of animal behavior. *Nature methods* 10, 1 (2013), 64–67.
- [80] Vadim Kantorov and Ivan Laptev. 2014. Efficient Feature Extraction, Encoding, and Classification for Action Recognition. In *2014 IEEE Conference on Computer Vision and Pattern Recognition (CVPR)*. IEEE Computer Society, Los Alamitos, CA, USA, 2593–2600. <https://doi.org/10.1109/CVPR.2014.332>
- [81] Pierre Karashchuk, Katie L. Rupp, Evynn S. Dickinson, Sarah Walling-Bell, Elischa Sanders, Eiman Azim, Bingni W. Brunton, and John C. Tuthill. 2021. Anipose: A toolkit for robust markerless 3D pose estimation. *Cell Reports* 36, 13 (2021), 109730. <https://doi.org/10.1016/j.celrep.2021.109730>
- [82] A. Karpathy, G. Toderici, S. Shetty, T. Leung, R. Sukthankar, and L. Fei-Fei. 2014. Large-Scale Video Classification with Convolutional Neural Networks. In *2014 IEEE Conference on Computer Vision and Pattern Recognition (CVPR)*. IEEE Computer Society, Los Alamitos, CA, USA, 1725–1732. <https://doi.org/10.1109/CVPR.2014.223>
- [83] Will Kay, João Carreira, Karen Simonyan, Brian Zhang, Chloe Hillier, Sudheendra Vijayanarasimhan, Fabio Viola, Tim Green, Trevor Back, Paul Natsev, Mustafa Suleyman, and Andrew Zisserman. 2017. The Kinetics Human Action Video Dataset. arXiv:1705.06950 <http://arxiv.org/abs/1705.06950>
- [84] Natasa Kleanthous, Abir Jaafar Hussain, Wasiq Khan, Jennifer Sneddon, Ahmed Al-Shamma'a, and Panos Liatsis. 2022. A survey of machine learning approaches in animal behaviour. *Neurocomputing* 491 (2022), 442–463. <https://doi.org/10.1016/j.neucom.2021.10.126>
- [85] Ugne Klibaite, Gordon Berman, Jessica Cande, David Stern, and Joshua Shaevitz. 2017. An unsupervised method for quantifying the behavior of paired animals. *Physical biology* 14 (01 2017). <https://doi.org/10.1088/1478-3975/aa5c50>
- [86] S Koncz, Z Gáll, and M Kolcsár. 2017. Measuring anxiety with behavior analysis software and comparing human observations with EthoVision XT in the elevated plus maze paradigm. *Acta Pharmaceutica Hungarica* 87, 1 (2017), 13–18.
- [87] Alex Krizhevsky and Geoffrey Hinton. 2009. *Learning multiple layers of features from tiny images*. Technical Report 0. University of Toronto, Toronto, Ontario.
- [88] Alex Krizhevsky, Ilya Sutskever, and Geoffrey E. Hinton. 2017. ImageNet Classification with Deep Convolutional Neural Networks. *Commun. ACM* 60, 6 (may 2017), 844–850. <https://doi.org/10.1145/3065386>
- [89] Ivan Laptev, Marcin Marszałek, Cordelia Schmid, and Benjamin Rozenfeld. 2008. Learning realistic human actions from movies. In *2008 IEEE Conference on Computer Vision and Pattern Recognition (CVPR)*. IEEE Computer Society, Los Alamitos, CA, USA, 1–8. <https://doi.org/10.1109/CVPR.2008.4587756>
- [90] Jessy Lauer, Mu Zhou, Shaokai Ye, William Menegas, Steffen Schneider, Tanmay Nath, Mohammed Mostafizur Rahman, Valentina Di Santo, Daniel Soberanes, Guoping Feng, Venkatesh N. Murthy, George Lauder, Catherine Dulac, Mackenzie Weygandt Mathis, and Alexander Mathis. 2022. Multi-animal pose estimation, identification and tracking with DeepLabCut. *Nature Methods* 19, 4 (01 Apr 2022), 496–504. <https://doi.org/10.1038/s41592-022-01443-0>
- [91] Van Anh Le and Kartikeya Murari. 2019. Recurrent 3D Convolutional Network for Rodent Behavior Recognition. In *ICASSP 2019 - 2019 IEEE International Conference on Acoustics, Speech and Signal Processing (ICASSP)*. IEEE, New York, NY, USA, 1174–1178. <https://doi.org/10.1109/ICASSP.2019.8683238>
- [92] Y. LeCun, B. Boser, J. S. Denker, D. Henderson, R. E. Howard, W. Hubbard, and L. D. Jackel. 1989. Backpropagation Applied to Handwritten Zip Code Recognition. *Neural Computation* 1, 4 (1989), 541–551. <https://doi.org/10.1162/neco.1989.1.4.541>
- [93] Y. Lecun, L. Bottou, Y. Bengio, and P. Haffner. 1998. Gradient-based learning applied to document recognition. *Proc. IEEE* 86, 11 (1998), 2278–2324. <https://doi.org/10.1109/5.726791>
- [94] Jingyuan Li, Moïshe Keselman, and Eli Shlizerman. 2022. OpenLabCluster: Active Learning Based Clustering and Classification of Animal Behaviors in Videos Based on Automatically Extracted Kinematic Body Keypoints. <https://doi.org/10.1101/2022.10.10.511660>
- [95] K. Li, S. Wang, X. Zhang, Y. Xu, W. Xu, and Z. Tu. 2021. Pose Recognition with Cascade Transformers. In *2021 IEEE/CVF Conference on Computer Vision and Pattern Recognition (CVPR)*. IEEE Computer Society, Los Alamitos, CA, USA, 1944–1953. <https://doi.org/10.1109/CVPR46437.2021.00198>
- [96] Sijin Li and Antoni B. Chan. 2015. 3D Human Pose Estimation from Monocular Images with Deep Convolutional Neural Network. In *Computer Vision – ACCV 2014*, Daniel Cremers, Ian Reid, Hideo Saito, and Ming-Hsuan Yang (Eds.). Springer International Publishing, Cham, 332–347.
- [97] Shufei Li, Junming Fan, Pai Zheng, and Lihui Wang. 2021. Transfer Learning-enabled Action Recognition for Human-robot Collaborative Assembly. *Procedia CIRP* 104 (2021), 1795–1800. <https://doi.org/10.1016/j.procir.2021.11.303> 54th CIRP CMS 2021 - Towards Digitalized Manufacturing 4.0.
- [98] Sijin Li, Weichen Zhang, and Antoni B. Chan. 2017. Maximum-Margin Structured Learning with Deep Networks for 3D Human Pose Estimation. *International Journal of Computer Vision* 122, 1 (01 Mar 2017), 149–168. <https://doi.org/10.1007/s11263-016-0962-x>
- [99] Yanshan Li, Rongjie Xia, Qinghua Huang, Weixin Xie, and Xuelong Li. 2017. Survey of Spatio-Temporal Interest Point Detection Algorithms in Video. *IEEE Access* 5 (2017), 10323–10331.
- [100] T. Lindeberg and I. Laptev. 2003. Space-time Interest Points. In *Computer Vision, IEEE International Conference on*, Vol. 2. IEEE Computer Society, Los Alamitos, CA, USA, 432. <https://doi.org/10.1109/ICCV.2003.1238378>
- [101] Malte Lorbach, Elisavet I Kyriakou, Ronald Poppe, Elsbeth A van Dam, Lucas PJJ Noldus, and Remco C Veltkamp. 2018. Learning to recognize rat social behavior: Novel dataset and cross-dataset application. *Journal of neuroscience methods* 300 (2018), 166–172.
- [102] Bruce D. Lucas and Takeo Kanade. 1981. An Iterative Image Registration Technique with an Application to Stereo Vision. In *Proceedings of the 7th International Joint Conference on Artificial Intelligence - Volume 2* (Vancouver, BC, Canada) (IJCAI'81). Morgan Kaufmann Publishers Inc., San Francisco, CA, USA, 674–679.
- [103] Yue Luo, Jimmy Ren, Zhouxia Wang, Wenxiu Sun, Jinshan Pan, Jianbo Liu, Jiahao Pang, and Liang Lin. 2018. LSTM Pose Machines. In *2018 IEEE/CVF Conference on Computer Vision and Pattern Recognition (CVPR)*. IEEE Computer Society, Los Alamitos, CA, USA, 5207–5215. <https://doi.org/10.1109/CVPR.2018.00546>
- [104] Andrew L. Maas. 2013. Rectifier Nonlinearities Improve Neural Network Acoustic Models. In *Proceedings of the 30th International Conference on Machine Learning - Volume 31*. PMLR, Atlanta, GA, USA, 3.
- [105] Markus Marks, Qiuhan Jin, Oliver Sturman, Lukas von Ziegler, Sepp Kollmorgen, Wolfgang von der Behrens, Valerio Mante, and Mehmet Fatih Hohacek, Johannes and Yanik. 2022. Deep-learning-based identification, tracking, pose estimation and behaviour classification of interacting primates and mice in complex environments. *Nature Machine Intelligence* 4, 4 (2022), 331–340.
- [106] Jesse D Marshall, Tianqing Li, Joshua H Wu, and Timothy W Dunn. 2022. Leaving flatland: Advances in 3D behavioral measurement. *Current Opinion in Neurobiology* 73 (2022), 102522.
- [107] J. Martinez, R. Hossain, J. Romero, and J. J. Little. 2017. A Simple Yet Effective Baseline for 3d Human Pose Estimation. In *2017 IEEE International Conference on Computer Vision (ICCV)*. IEEE Computer Society, Los Alamitos, CA, USA, 2659–2668. <https://doi.org/10.1109/ICCV.2017.288>
- [108] Alexander Mathis, Pranav Mamidanna, Kevin M. Cury, Taiga Abe, Venkatesh N. Murthy, Mackenzie Weygandt Mathis, and Matthias Bethge. 2018. DeepLabCut: markerless pose estimation of user-defined body parts with deep learning. *Nature Neuroscience* 21, 9 (2018), 1281–1289. <https://doi.org/10.1038/s41593-018-0209-y>
- [109] Mackenzie Weygandt Mathis and Alexander Mathis. 2020. Deep learning tools for the measurement of animal behavior in neuroscience. *Current Opinion in Neurobiology* 60 (2020), 1–11. <https://doi.org/10.1016/j.conb.2019.10.008> Neurobiology of Behavior.
- [110] Warren McCulloch and Walter Pitts. 1943. A Logical Calculus of Ideas Immanent in Nervous Activity. *Bulletin of Mathematical Biophysics* 5 (1943), 127–147.
- [111] Leland McInnes, John Healy, and James Melville. 2018. UMAP: Uniform Manifold Approximation and Projection for Dimension Reduction. <http://arxiv.org/abs/1802.03426> cite arxiv:1802.03426Comment: Reference implementation available at <http://github.com/lmcinnes/umap>
- [112] D. Mehta, H. Rhodin, D. Casas, P. Fua, O. Sotnychenko, W. Xu, and C. Theobalt. 2017. Monocular 3D Human Pose Estimation in the Wild Using Improved CNN Supervision. In *2017 International Conference on 3D Vision (3DV)*. IEEE Computer Society, Los Alamitos, CA, USA, 506–516. <https://doi.org/10.1109/3DV.2017.00064>
- [113] Fernand Meyer. 1994. Topographic distance and watershed lines. *Signal processing* 38, 1 (1994), 113–125.
- [114] Sara Moccia, Lucia Migliorelli, Virgilio Carnielli, and Emanuele Frontoni. 2019. Preterm infants’s pose estimation with spatio-temporal features. *IEEE Transactions on Biomedical Engineering* 67, 8 (2019), 2370–2380.
- [115] Kevin P. Murphy. 2012. *Machine Learning: A Probabilistic Perspective*. The MIT Press, Cambridge, MA, USA.
- [116] Tanmay Nath, Alexander Mathis, An Chi Chen, Amir Patel, Matthias Bethge, and Mackenzie Weygandt Mathis. 2019. Using DeepLabCut for 3D markerless pose estimation across species and behaviors. *Nature Protocols* 14, 7 (01 Jul 2019), 2152–2176. <https://doi.org/10.1038/s41596-019-0176-0>
- [117] Yuval Netzer, Tao Wang, Adam Coates, Alessandro Bissacco, Bo Wu, and Andrew Y. Ng. 2011. Reading Digits in Natural Images with Unsupervised Feature Learning.
- [118] Alejandro Newell, Kaiyu Yang, and Jia Deng. 2016. Stacked Hourglass Networks for Human Pose Estimation. In *Computer Vision – ECCV 2016*, Bastian Leibe, Jiri Matas, Nicu Sebe, and Max Welling (Eds.). Springer International Publishing, Cham, 483–499.
- [119] J. Ng, J. Choi, J. Neumann, and L. S. Davis. 2018. ActionFlowNet: Learning Motion Representation for Action Recognition. In *2018 IEEE Winter Conference on Applications of Computer Vision (WACV)*. IEEE Computer Society, Los Alamitos,

- CA, USA, 1616–1624. <https://doi.org/10.1109/WACV.2018.00179>
- [120] Ngoc Giang Nguyen, Dau Phan, Favorisen Rosyking Lumbanraja, Mohammad Reza Faisal, Bahridin Abapihi, Bedy Purnama, Kunti Robiatul Delimayanti, Mera Kartikaand Mahmudah, Mamoru Kubo, and Kenji Satou. 2019. Applying deep learning models to mouse behavior recognition. *Journal of Biomedical Science and Engineering* 12, 02 (2019), 183–196.
- [121] Simon RO Nilsson, Nastacia Goodwin, Jia Jie Choong, Sophia Hwang, Hayden Wright, Zane Norville, Xiaoyu Tong, Dayu Lin, Brandon Bentzley, Neir Eshel, Ryan McLaughlin, and Sam Golden. 2020. Simple Behavioral Analysis (SimBA) – An open source toolkit for computer classification of complex social behaviors in experimental animals. (2020). <https://doi.org/10.1101/2020.04.19.049452>
- [122] Noldus Information Technology. 2011. EthoVision XT 8.0. <http://www.noldus.com/ethovision>
- [123] Shay Ohayon, Ofer Avni, Adam L. Taylor, Pietro Perona, and S.E. Roian Egnor. 2013. Automated multi-day tracking of marked mice for the analysis of social behaviour. *Journal of Neuroscience Methods* 219, 1 (2013), 10–19. <https://doi.org/10.1016/j.jneumeth.2013.05.013>
- [124] Maxime Oquab, Leon Bottou, Ivan Laptev, and Josef Sivic. 2014. Learning and Transferring Mid-Level Image Representations Using Convolutional Neural Networks. In *Proceedings of the 2014 IEEE Conference on Computer Vision and Pattern Recognition (CVPR '14)*. IEEE Computer Society, USA, 1717–1724. <https://doi.org/10.1109/CVPR.2014.222>
- [125] G. Pavlakos, X. Zhou, K. G. Derpanis, and K. Daniilidis. 2017. Coarse-to-Fine Volumetric Prediction for Single-Image 3D Human Pose. In *2017 IEEE Conference on Computer Vision and Pattern Recognition (CVPR)*. IEEE Computer Society, Los Alamitos, CA, USA, 1263–1272. <https://doi.org/10.1109/CVPR.2017.139>
- [126] Judea Pearl. 1982. Reverend Bayes on Inference Engines: A Distributed Hierarchical Approach. In *Proceedings of the Second AAAI Conference on Artificial Intelligence (Pittsburgh, Pennsylvania) (AAAI'82)*. AAAI Press, Washington, DC, USA, 133–136.
- [127] Xiaojiang Peng, Limin Wang, Xingxing Wang, and Yu Qiao. 2016. Bag of visual words and fusion methods for action recognition: Comprehensive study and good practice. *Computer Vision and Image Understanding* 150 (2016), 109–125. <https://doi.org/10.1016/j.cviu.2016.03.013>
- [128] Talmo D Pereira, Diego E Aldarondo, Lindsay Willmore, Mikhail Kislin, Samuel S-H Wang, Mala Murthy, and Joshua W Shaevitz. 2019. Fast animal pose estimation using deep neural networks. *Nature methods* 16, 1 (2019), 117–125.
- [129] Talmo D. Pereira, Nathaniel Tabris, Arie Matsliah, David M. Turner, Junyu Li, Shruthi Ravindranath, Eleni S. Papadopyannis, Edna Normand, David S. Deutsch, Z. Yan Wang, Grace C. McKenzie-Smith, Catalin C. Mitelut, Marielisa Diez Castro, John D'Uva, Mikhail Kislin, Dan H. Sanes, Sarah D. Kocher, Samuel S.-H. Wang, Annegret L. Falkner, Joshua W. Shaevitz, and Mala Murthy. 2022. SLEAP: A deep learning system for multi-animal pose tracking. *Nature Methods* 19, 4 (01 Apr 2022), 486–495. <https://doi.org/10.1038/s41592-022-01426-1>
- [130] T. Pfister, J. Charles, and A. Zisserman. 2015. Flowing ConvNets for Human Pose Estimation in Videos. In *2015 IEEE International Conference on Computer Vision (ICCV)*. IEEE Computer Society, Los Alamitos, CA, USA, 1913–1921. <https://doi.org/10.1109/ICCV.2015.222>
- [131] Tomas Pfister, Karen Simonyan, James Charles, and Andrew Zisserman. 2015. Deep Convolutional Neural Networks for Efficient Pose Estimation in Gesture Videos. In *Computer Vision – ACCV 2014*, Daniel Cremers, Ian Reid, Hideo Saito, and Ming-Hsuan Yang (Eds.). Springer International Publishing, Cham, 538–552.
- [132] Aj Piergiovanni and Michael Ryoo. 2019. Temporal Gaussian Mixture Layer for Videos. In *Proceedings of the 36th International Conference on Machine Learning (Proceedings of Machine Learning Research)*, Kamalika Chaudhuri and Ruslan Salakhutdinov (Eds.), Vol. 97. PMLR, Long Beach, California, USA, 5152–5161. <https://proceedings.mlr.press/v97/piergiovanni19a.html>
- [133] L. Pishchulin, E. Insafutdinov, S. Tang, B. Andres, M. Andriluka, P. Gehler, and B. Schiele. 2016. DeepCut: Joint Subset Partition and Labeling for Multi Person Pose Estimation. In *2016 IEEE Conference on Computer Vision and Pattern Recognition (CVPR)*. IEEE Computer Society, Los Alamitos, CA, USA, 4929–4937. <https://doi.org/10.1109/CVPR.2016.533>
- [134] Joseph Redmon and Ali Farhadi. 2018. YOLOv3: An Incremental Improvement. <https://doi.org/10.48550/ARXIV.1804.02767>
- [135] Stacey Reynolds, Meagan Urruela, and Darragh P Devine. 2013. Effects of environmental enrichment on repetitive behaviors in the BTBR T+tf/mj mouse model of autism. *Autism Research* 6, 5 (2013), 337–343.
- [136] Olaf Ronneberger, Philipp Fischer, and Thomas Brox. 2015. U-Net: Convolutional Networks for Biomedical Image Segmentation. In *Medical Image Computing and Computer-Assisted Intervention – MICCAI 2015*, Nassir Navab, Joachim Hornegger, William M. Wells, and Alejandro F. Frangi (Eds.). Springer International Publishing, Cham, 234–241.
- [137] J. Rousseau, P. Lochem, W. Gispen, and Berry Spruijt. 2000. Classification of rat behavior with an image-processing method and a neural network. *Behavior research methods, instruments, & computers: a journal of the Psychonomic Society, Inc* 32 (03 2000), 63–71. <https://doi.org/10.3758/BF03200789>
- [138] B. Sapp and B. Taskar. 2013. MODEC: Multimodal Decomposable Models for Human Pose Estimation. In *2013 IEEE Conference on Computer Vision and Pattern Recognition (CVPR)*. IEEE Computer Society, Los Alamitos, CA, USA, 3674–3681. <https://doi.org/10.1109/CVPR.2013.471>
- [139] Cristina Segalin, Jalani Williams, Tomomi Karigo, May Hui, Moriel Zelikowsky, Jennifer J Sun, Pietro Perona, David J Anderson, and Ann Kennedy. 2021. The Mouse Action Recognition System (MARS) software pipeline for automated analysis of social behaviors in mice. *eLife* 10 (nov 2021), e63720. <https://doi.org/10.7554/eLife.63720>
- [140] Leonid Sigal, Alexandru Balan, and Michael Black. 2010. HumanEva: Synchronized Video and Motion Capture Dataset and Baseline Algorithm for Evaluation of Articulated Human Motion. *International Journal of Computer Vision* 87 (03 2010), 4–27. <https://doi.org/10.1007/s11263-009-0273-6>
- [141] Karen Simonyan and Andrew Zisserman. 2014. Two-Stream Convolutional Networks for Action Recognition in Videos. In *Proceedings of the 27th International Conference on Neural Information Processing Systems - Volume 1 (Montreal, Canada) (NIPS'14)*. MIT Press, Cambridge, MA, USA, 568–576.
- [142] Karen Simonyan and Andrew Zisserman. 2015. Very deep convolutional networks for large-scale image recognition. In 3rd International Conference on Learning Representations (ICLR 2015). *3rd International Conference on Learning Representations (ICLR 2015)* 3, 1–14.
- [143] Khurram Soomro, Amir Roshan Zamir, and Mubarak Shah. 2012. UCF101: A Dataset of 101 Human Actions Classes From Videos in The Wild. arXiv:1212.0402 <http://arxiv.org/abs/1212.0402>
- [144] Greg J. Stephens, Bethany Johnson-Kerner, William Bialek, and William . Ryu. 2008. Dimensionality and Dynamics in the Behavior of C. elegans. *PLOS Computational Biology* 4, 4 (04 2008), 1–10. <https://doi.org/10.1371/journal.pcbi.1000028>
- [145] Russell Stewart, Mykhaylo Andriluka, and Andrew Y. Ng. 2016. End-to-End People Detection in Crowded Scenes. In *2016 IEEE Conference on Computer Vision and Pattern Recognition (CVPR)*. IEEE Computer Society, Los Alamitos, CA, USA, 2325–2333. <https://doi.org/10.1109/CVPR.2016.255>
- [146] Oliver Sturman, Lukas von Ziegler, Christa Schläppi, Furkan Akyol, Mattia Privitera, Daria Slominski, Christina Grimm, Laetitia Thieren, Valerio Zerbi, Benjamin Grewe, and Johannes Bohacek. 2020. Deep learning-based behavioral analysis reaches human accuracy and is capable of outperforming commercial solutions. *Neuropsychopharmacology* 45, 11 (01 Oct 2020), 1942–1952. <https://doi.org/10.1038/s41386-020-0776-y>
- [147] Joshua Susskind, Adam Anderson, and Geoffrey E Hinton. 2010. *The Toronto face dataset*. Technical Report. Technical Report UTM TR 2010-001, U. Toronto.
- [148] C. Szegedy, Wei Liu, Yangqing Jia, P. Sermanet, S. Reed, D. Anguelov, D. Erhan, V. Vanhoucke, and A. Rabinovich. 2015. Going deeper with convolutions. In *2015 IEEE Conference on Computer Vision and Pattern Recognition (CVPR)*. IEEE Computer Society, Los Alamitos, CA, USA, 1–9. <https://doi.org/10.1109/CVPR.2015.7298594>
- [149] C. Szegedy, V. Vanhoucke, S. Ioffe, J. Shlens, and Z. Wojna. 2016. Rethinking the Inception Architecture for Computer Vision. In *2016 IEEE Conference on Computer Vision and Pattern Recognition (CVPR)*. IEEE Computer Society, Los Alamitos, CA, USA, 2818–2826. <https://doi.org/10.1109/CVPR.2016.308>
- [150] Mingxing Tan and Quoc Le. 2019. EfficientNet: Rethinking Model Scaling for Convolutional Neural Networks. In *Proceedings of the 36th International Conference on Machine Learning (Proceedings of Machine Learning Research)*, Kamalika Chaudhuri and Ruslan Salakhutdinov (Eds.), Vol. 97. PMLR, Long Beach, California, USA, 6105–6114. <https://proceedings.mlr.press/v97/tan19a.html>
- [151] B. Tekin, A. Rozantsev, V. Lepetit, and P. Fua. 2016. Direct Prediction of 3D Body Poses from Motion Compensated Sequences. In *2016 IEEE Conference on Computer Vision and Pattern Recognition (CVPR)*. IEEE Computer Society, Los Alamitos, CA, USA, 991–1000. <https://doi.org/10.1109/CVPR.2016.113>
- [152] D. Tome, C. Russell, and L. Agapito. 2017. Lifting from the Deep: Convolutional 3D Pose Estimation from a Single Image. In *2017 IEEE Conference on Computer Vision and Pattern Recognition (CVPR)*. IEEE Computer Society, Los Alamitos, CA, USA, 5689–5698. <https://doi.org/10.1109/CVPR.2017.603>
- [153] J. Tompson, R. Goroshin, A. Jain, Y. LeCun, and C. Bregler. 2015. Efficient object localization using Convolutional Networks. In *2015 IEEE Conference on Computer Vision and Pattern Recognition (CVPR)*. IEEE Computer Society, Los Alamitos, CA, USA, 648–656. <https://doi.org/10.1109/CVPR.2015.7298664>
- [154] Jonathan Tompson, Arjun Jain, Yann LeCun, and Christoph Bregler. 2014. Joint Training of a Convolutional Network and a Graphical Model for Human Pose Estimation. In *Proceedings of the 27th International Conference on Neural Information Processing Systems - Volume 1 (Montreal, Canada) (NIPS'14)*. MIT Press, Cambridge, MA, USA, 1799–1807.
- [155] A. Toshev and C. Szegedy. 2014. DeepPose: Human Pose Estimation via Deep Neural Networks. In *2014 IEEE Conference on Computer Vision and Pattern Recognition (CVPR)*. IEEE Computer Society, Los Alamitos, CA, USA, 1653–1660. <https://doi.org/10.1109/CVPR.2014.214>

- [156] D. Tran, L. Bourdev, R. Fergus, L. Torresani, and M. Paluri. 2015. Learning Spatiotemporal Features with 3D Convolutional Networks. In *2015 IEEE International Conference on Computer Vision (ICCV)*. IEEE Computer Society, Los Alamitos, CA, USA, 4489–4497. <https://doi.org/10.1109/ICCV.2015.510>
- [157] D. Tran, H. Wang, L. Torresani, J. Ray, Y. LeCun, and M. Paluri. 2018. A Closer Look at Spatiotemporal Convolutions for Action Recognition. In *2018 IEEE/CVF Conference on Computer Vision and Pattern Recognition (CVPR)*. IEEE Computer Society, Los Alamitos, CA, USA, 6450–6459. <https://doi.org/10.1109/CVPR.2018.00675>
- [158] B. Triggs and N. Dalal. 2005. Histograms of Oriented Gradients for Human Detection. In *2013 IEEE Conference on Computer Vision and Pattern Recognition*, Vol. 2. IEEE Computer Society, Los Alamitos, CA, USA, 886–893. <https://doi.org/10.1109/CVPR.2005.177>
- [159] E. Vahdani and Y. Tian. 2022. Deep Learning-based Action Detection in Untrimmed Videos: A Survey. *IEEE Transactions on Pattern Analysis and Machine Intelligence* (jul 2022), 1–20. <https://doi.org/10.1109/TPAMI.2022.3193611>
- [160] Elsbeth A van Dam, Lucas PJJ Noldus, and Marcel AJ van Gerven. 2020. Deep learning improves automated rodent behavior recognition within a specific experimental setup. *Journal of neuroscience methods* 332 (2020), 108536.
- [161] Elsbeth A van Dam, Johanneke E van der Harst, Cajo JF ter Braak, Ruud AJ Tegelebosch, Berry M Spruijt, and Lucas PJJ Noldus. 2013. An automated system for the recognition of various specific rat behaviours. *Journal of neuroscience methods* 218, 2 (2013), 214–224.
- [162] Aaron van den Oord, Sander Dieleman, Heiga Zen, Karen Simonyan, Oriol Vinyals, Alex Graves, Nal Kalchbrenner, Andrew Senior, and Koray Kavukcuoglu. 2016. WaveNet: A Generative Model for Raw Audio. , 125–125 pages.
- [163] Laurens van der Maaten and Geoffrey Hinton. 2008. Visualizing Data using t-SNE. *Journal of Machine Learning Research* 9, 86 (2008), 2579–2605. <http://jmlr.org/papers/v9/vandermaten08a.html>
- [164] Ashish Vaswani, Noam Shazeer, Niki Parmar, Jakob Uszkoreit, Llion Jones, Aidan N. Gomez, Lukasz Kaiser, and Illia Polosukhin. 2017. Attention is All You Need. In *Proceedings of the 31st International Conference on Neural Information Processing Systems (Long Beach, California, USA) (NIPS'17)*. Curran Associates Inc., Red Hook, NY, USA, 6000–6010.
- [165] Joshua T. Vogelstein, Youngser Park, Tomoko Ohyama, Rex A. Kerr, James W. Truman, Carey E. Priebe, and Marta Zlatić. 2014. Discovery of Brain-wide Neural-Behavioral Maps via Multiscale Unsupervised Structure Learning. *Science* 344, 6182 (2014), 386–392. <https://doi.org/10.1126/science.1250298> arXiv:<https://www.science.org/doi/pdf/10.1126/science.1250298>
- [166] Lukas von Ziegler, Oliver Sturman, and Johannes Bohacek. 2021. Big behavior: challenges and opportunities in a new era of deep behavior profiling. *Neuropsychopharmacology* 46, 1 (2021), 33–44.
- [167] Heng Wang, A. Klaser, C. Schmid, and Cheng-Lin Liu. 2011. Action Recognition by Dense Trajectories. In *Proceedings of the 2011 IEEE Conference on Computer Vision and Pattern Recognition (CVPR '11)*. IEEE Computer Society, USA, 3169–3176. <https://doi.org/10.1109/CVPR.2011.5995407>
- [168] H. Wang and C. Schmid. 2013. Action Recognition with Improved Trajectories. In *2013 IEEE International Conference on Computer Vision (ICCV)*. IEEE Computer Society, Los Alamitos, CA, USA, 3551–3558. <https://doi.org/10.1109/ICCV.2013.441>
- [169] Limin Wang, Yuanjun Xiong, Zhe Wang, Yu Qiao, Dahua Lin, Xiaoou Tang, and Luc Van Gool. 2016. Temporal Segment Networks: Towards Good Practices for Deep Action Recognition. In *Computer Vision – ECCV 2016*, Bastian Leibe, Jiri Matas, Nicu Sebe, and Max Welling (Eds.). Springer International Publishing, Cham, 20–36.
- [170] Shih-En Wei, Varun Ramakrishna, Takeo Kanade, and Yaser Sheikh. 2016. Convolutional pose machines. In *Proceedings of the IEEE conference on Computer Vision and Pattern Recognition*. IEEE Computer Society, USA, 4724–4732.
- [171] Alexander Wilschko, Tatsuya Tsukahara, Ayman Zeine, Rockwell Anyoha, Winthrop Gillis, Jeffrey Markowitz, Ralph Peterson, Jesse Katon, Matthew Johnson, and Sandeep Datta. 2020. Revealing the structure of pharmacobehavioral space through motion sequencing. *Nature Neuroscience* 23 (11 2020), 1–11. <https://doi.org/10.1038/s41593-020-00706-3>
- [172] Alexander B. Wilschko, Matthew J. Johnson, Giuliano Iurilli, Ralph E. Peterson, Jesse M. Katon, Stan L. Pashkovski, Victoria E. Abaira, Ryan P. Adams, and Sandeep Robert Datta. 2015. Mapping Sub-Second Structure in Mouse Behavior. *Neuron* 88, 6 (2015), 1121 – 1135. <https://doi.org/10.1016/j.neuron.2015.11.031>
- [173] Bing Xu, Naiyan Wang, Tianqi Chen, and Mu Li. 2015. Empirical Evaluation of Rectified Activations in Convolutional Network. arXiv:1505.00853 <http://arxiv.org/abs/1505.00853>
- [174] C. Zach, T. Pock, and H. Bischof. 2007. A Duality Based Approach for Realtime TV-L1 Optical Flow. In *Proceedings of the 29th DAGM Conference on Pattern Recognition* (Heidelberg, Germany). Springer-Verlag, Berlin, Heidelberg, 214–223.
- [175] B. Zhang, L. Wang, Z. Wang, Y. Qiao, and H. Wang. 2016. Real-Time Action Recognition with Enhanced Motion Vector CNNs. In *2016 IEEE Conference on Computer Vision and Pattern Recognition (CVPR)*. IEEE Computer Society, Los Alamitos, CA, USA, 2718–2726. <https://doi.org/10.1109/CVPR.2016.297>
- [176] Qingchao Zhang, Coy D. Heldermon, and Corey Toler-Franklin. 2020. Multiscale Detection of Cancerous Tissue in High Resolution Slide Scans. In *Advances in Visual Computing*, George Bebis, Zhaozheng Yin, Edward Kim, Jan Bender, Kartic Subr, Bum Chul Kwon, Jian Zhao, Denis Kalkofen, and George Baciu (Eds.). Springer International Publishing, Cham, 139–153.
- [177] Ce Zheng, Wenhan Wu, Taojiannan Yang, Sijie Zhu, Chen Chen, Ruixu Liu, Ju Shen, Nasser Kehtarnavaz, and Mubarak Shah. 2020. Deep Learning-Based Human Pose Estimation: A Survey. arXiv:2012.13392 <https://arxiv.org/abs/2012.13392>
- [178] Feixiang Zhou, Xinyu Yang, Fang Chen, Long Chen, Zheheng Jiang, Hui Zhu, Reiko Heckel, Haikuan Wang, Minrui Fei, and Huiyu Zhou. 2022. Cross-Skeleton Interaction Graph Aggregation Network for Representation Learning of Mouse Social Behaviour.
- [179] Tianxun Zhou, Calvin Chee Hoe Cheah, Eunice Wei Mun Chin, Jie Chen, Hui Jia Farm, Eyleen Lay Keow Goh, and Keng Hwee Chiam. 2022. Contrastive-Pose: A contrastive learning approach for self-supervised feature engineering for pose estimation and behavioral classification of interacting animals. <https://doi.org/10.1101/2022.11.09.515746>
- [180] Yi Zhu, Zhenzhong Lan, Shawn Newsam, and Alexander Hauptmann. 2019. Hidden Two-Stream Convolutional Networks for Action Recognition. In *Computer Vision – ACCV 2018*, C. V. Jawahar, Hongdong Li, Greg Mori, and Konrad Schindler (Eds.). Springer International Publishing, Cham, 363–378.
- [181] Yi Zhu, Xinyu Li, Chunhui Liu, Mohammadreza Zolfaghari, Yuanjun Xiong, Chongruo Wu, Zhi Zhang, Joseph Tighe, R. Manmatha, and Mu Li. 2020. A Comprehensive Study of Deep Video Action Recognition. arXiv:2012.06567 <https://arxiv.org/abs/2012.06567>